

Electrical scanning probe microscopy approaches to investigate solar cell junctions and devices

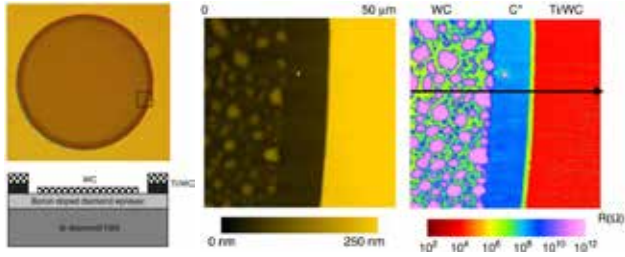
José Alvarez^{1,2,3}, Clément Marchat^{1,2,3}, Audrey Morisset^{1,2,3,4}, Letian Dai^{1,2,5,6},
Jean-Paul Kleider^{1,2,3}, Raphaël Cabal⁴, Pere Roca i Cabarrocas⁶

¹*Université Paris-Saclay, CentraleSupélec, CNRS, Laboratoire de Génie Electrique et Electronique de Paris (GeePs);*

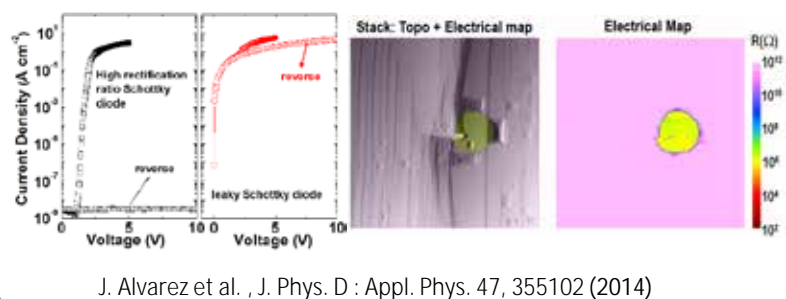
²*Sorbonne Université, CNRS, GeePs; ³Institut Photovoltaïque d'Ile-de-France (IPVF); ⁴Laboratory of Homojunction Solar Cells, Institute of Technologies for New Energies (CEA-Liten); ⁵Laboratoire de Physique de la Matière Condensée (LPMC), École Polytechnique; ⁶Laboratoire de Physique des Interfaces et des Couches Minces (LPICM), CNRS, Ecole Polytechnique*

High power and high temperature devices

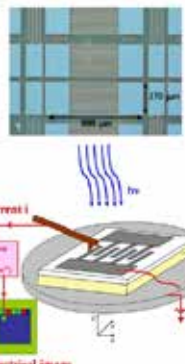
WC Schottky diode on homoepi. Diamond



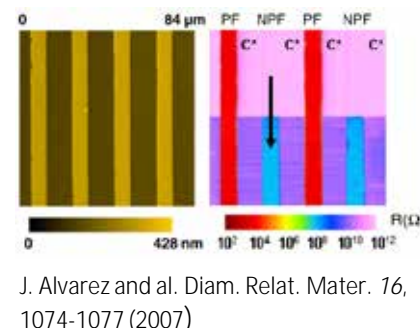
Evidencing leakage current in diamond Schottky devices



Deep UV photodetection

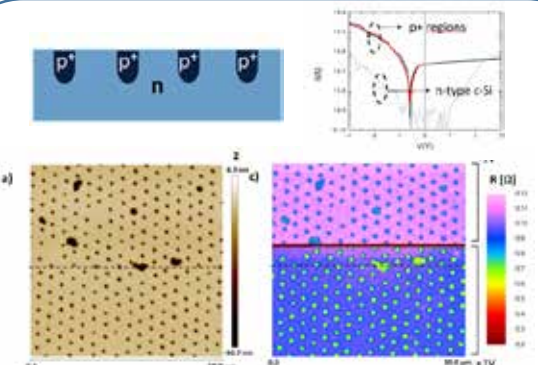


MSM Diamond photodetectors

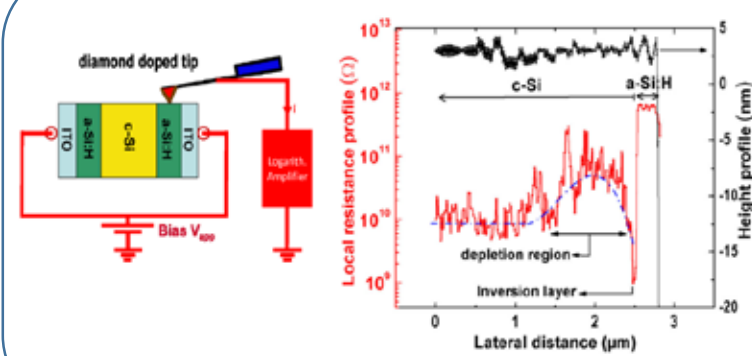


Energy harvesting

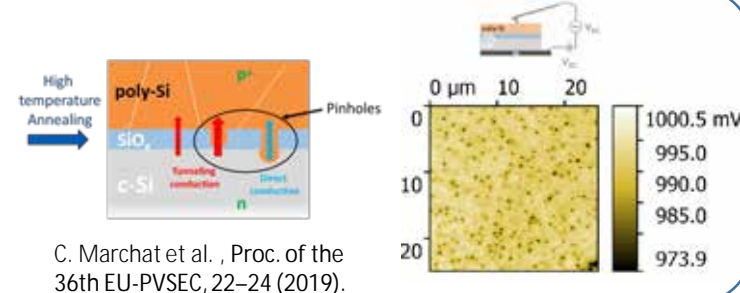
Nanodoping and evidencing PV effect



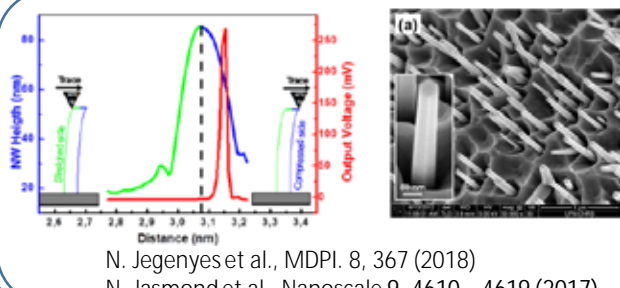
Cross-sectional analyses of a-Si:H/c-Si heterojunction



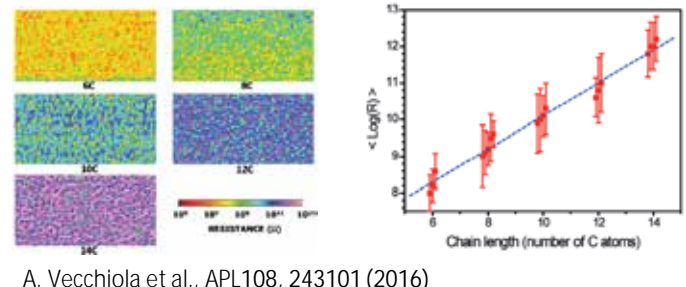
Polysilicon passivating contact structures



Piezoelectric Conversion of Axial InGaN/GaN NWs

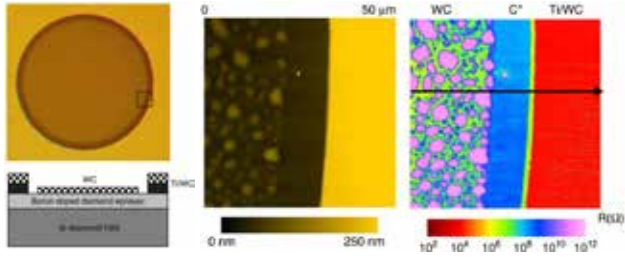


Self-assembled monolayers



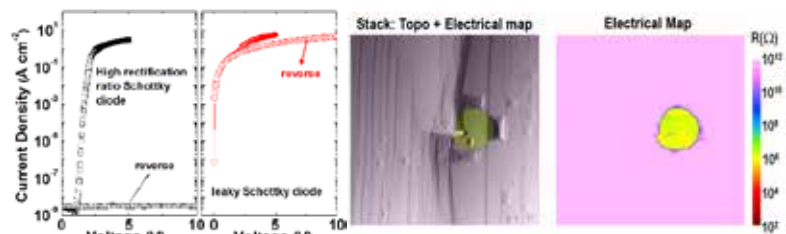
High power and high temperature devices

WC Schottky diode on homoepi. Diamond



J. Alvarez and al. *Superlattice Microst.* 40, 343-349 (2006)

Evidencing leakage current in diamond Schottky devices

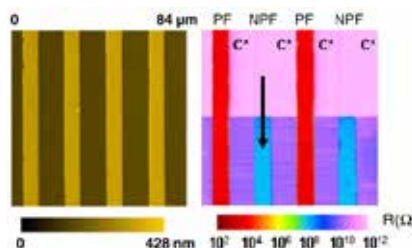


J. Alvarez et al. , *J. Phys. D : Appl. Phys.* 47, 355102 (2014)

Deep UV photodetection



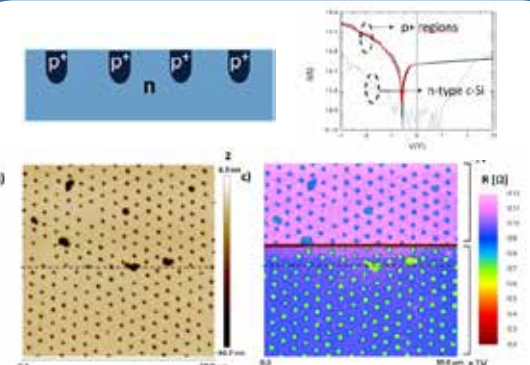
MSM Diamond photodetectors



J. Alvarez and al. *Diam. Relat. Mater.* 16, 1074-1077 (2007)

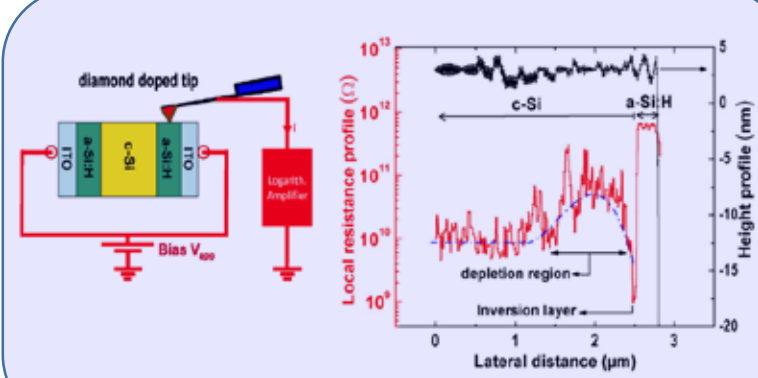
Energy harvesting

Nanodoping and evidencing PV effect



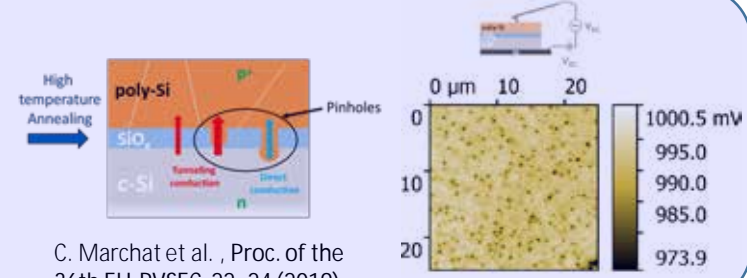
R. Khoury et al. , *Nano letters*, submitted (2020)

Cross-sectional analyses of a-Si:H/c-Si heterojunction



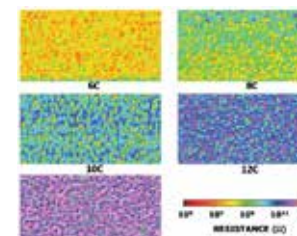
J.-P. Kleider et al. , *Phys. Status Solidi A* 216, &800877, (2019)

Polysilicon passivating contact structures



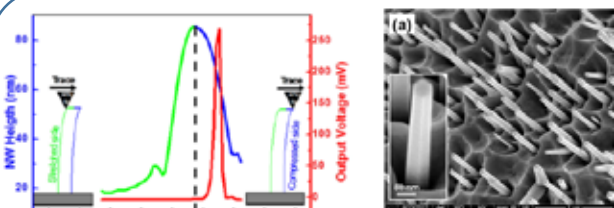
C. Marchat et al. , *Proc. of the 36th EU-PVSEC*, 22-24 (2019).

Self-assembled monolayers



A. Vecchiola et al., *APL108*, 243101 (2016)

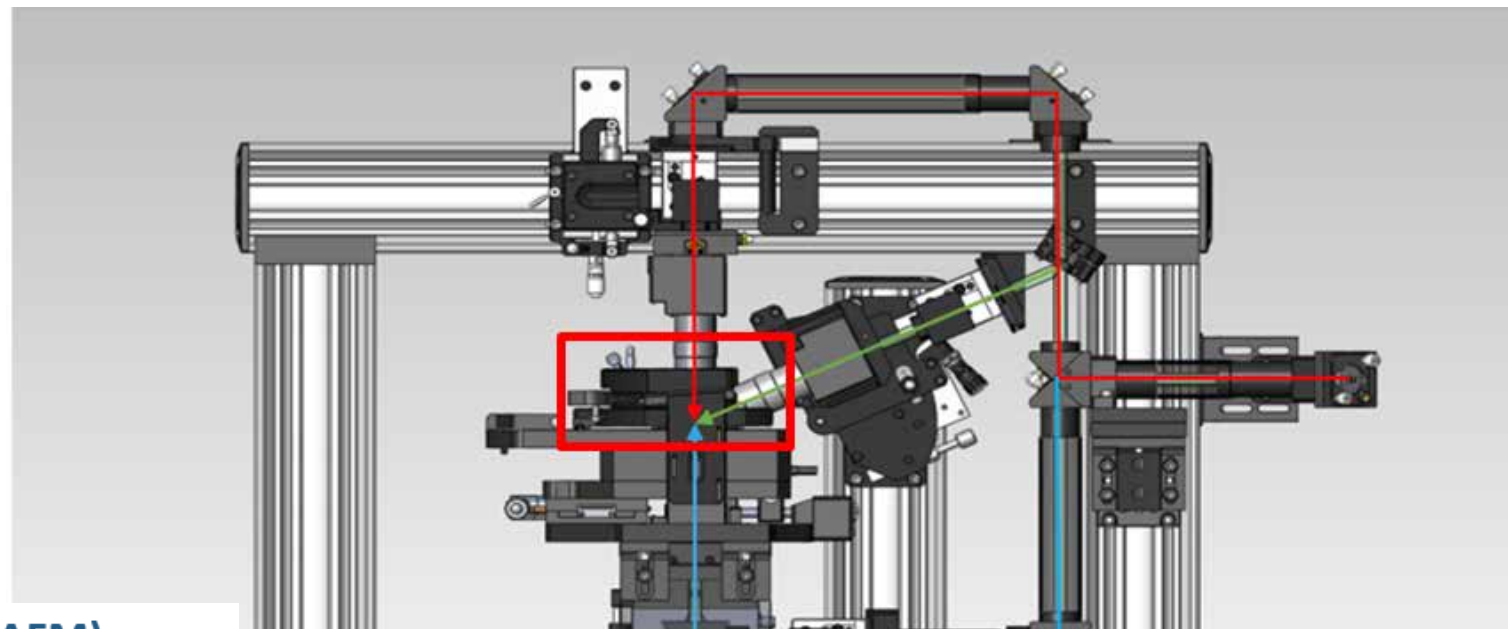
Piezoelectric Conversion of Axial InGaN/GaN NWs



N. Jegenyes et al., *MDPI* 8, 367 (2018)

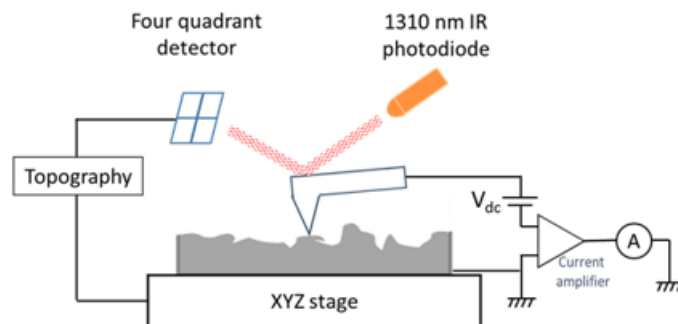
N. Jasmond et al., *Nanoscale* 9, 4610 – 4619 (2017)

Atomic Force Microscopy (AFM) setup



Conductive AFM (C-AFM):

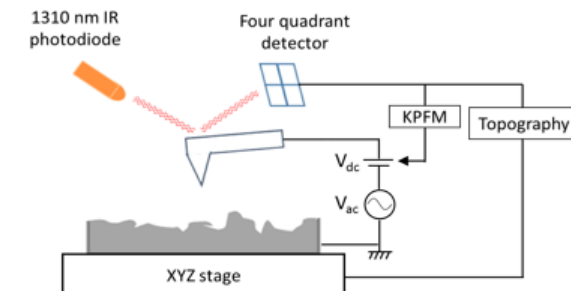
- local current and photocurrent mapping



AIST-NT/HORIBA

Kelvin probe force microscopy (KPFM) :

- contact potential difference (CPD) and surface photovoltage (SPV) mapping

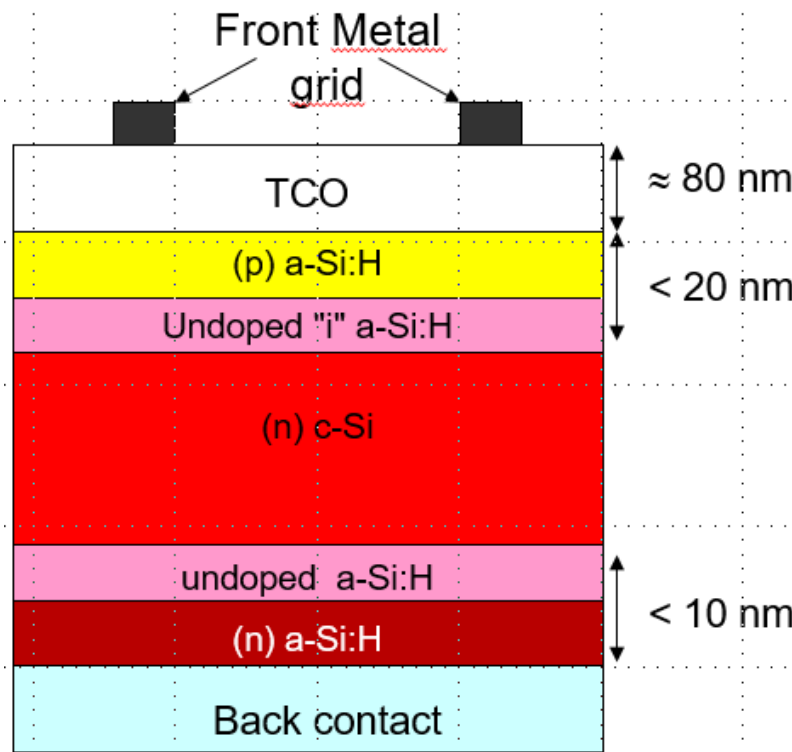


Part 1 - Hydrogenated amorphous silicon/crystalline silicon heterojunction

Part 2 - Passivating selective contacts: (p+) Poly-Si/SiO_x/c-Si

Part 3 - P-I-N radial junctions (RJ) Silicon Nanowires (SiNWs)

Hydrogenated amorphous silicon/crystalline silicon heterojunction



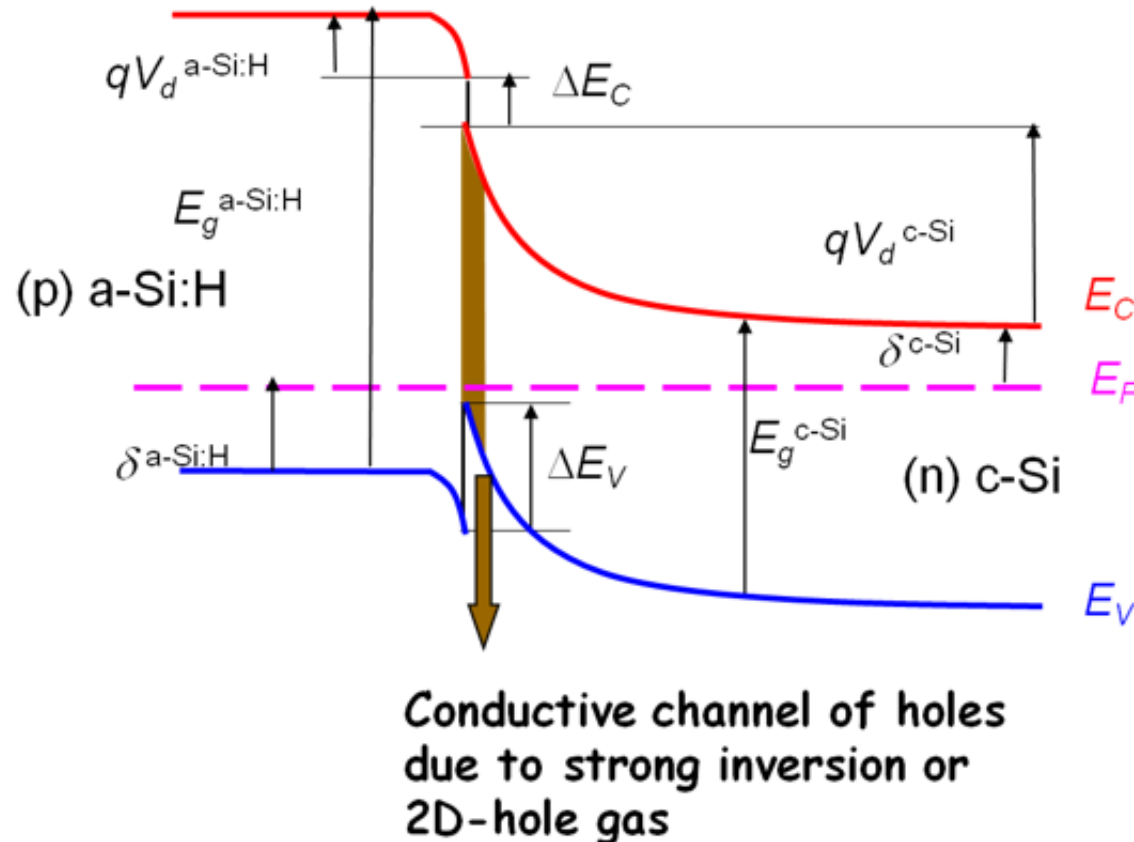
- § a-Si:H/c-Si Heterojunction solar cells “Si-HET” was first studied by Sanyo in the 80's [1]
- § Reducing recombination at the interfaces Si-HET has achieved the highest efficiency for c-Si tech. : 26.3-26.7% [2,3]

[1] Hamakawa et al. , Appl. Phys. Lett. 43, 644 (1983)

[2] Yoshikawa et al. , Nat. Energy 2, 17032 (2017)

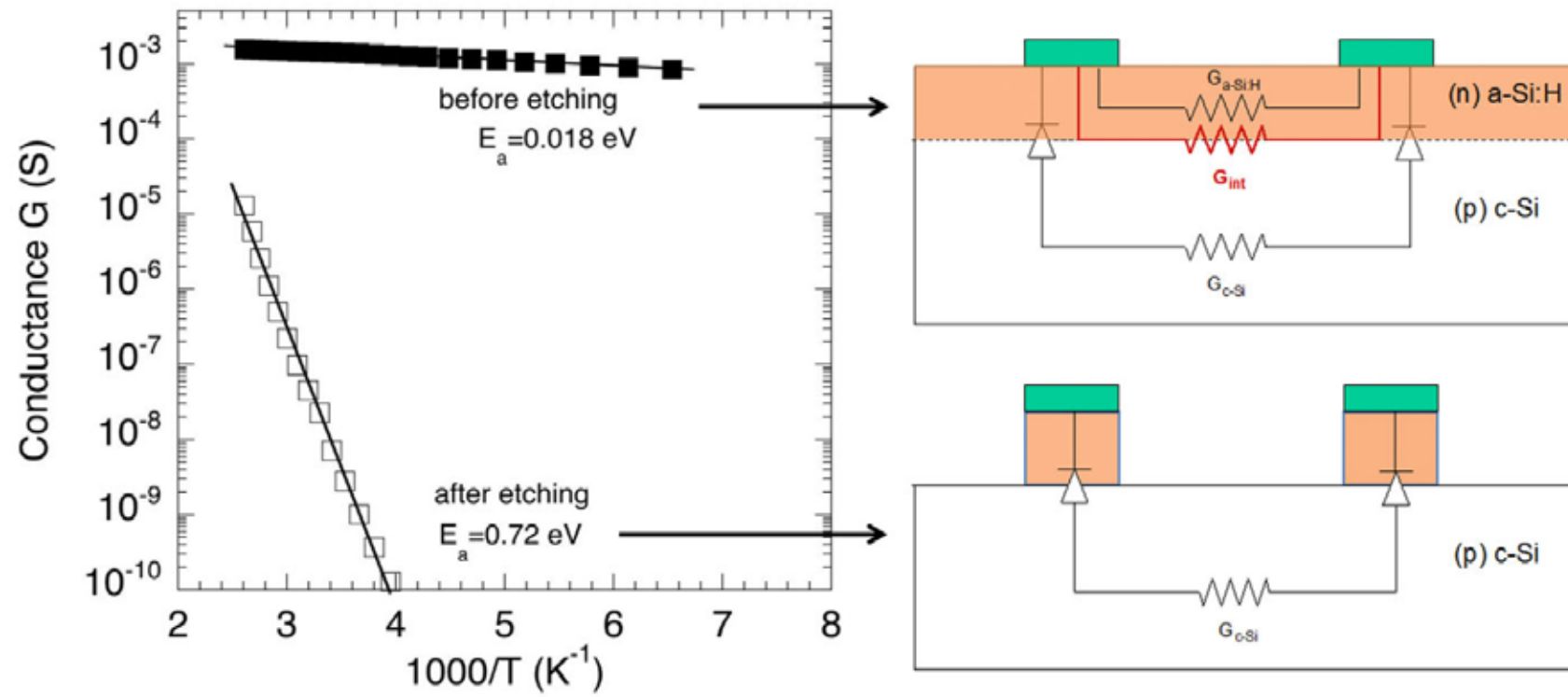
[3] Yamamoto et al. , Japan. J. Appl. Phys. 57, 08RB20 (2018)

1.1 Motivation : Interface Band lineup



§ a-Si:H/c-Si (N/p or P/n) studied by capacitance and planar conductance measurements suggest the presence of a strong inversion layer at the interface

1.2 Lateral conductance measurements

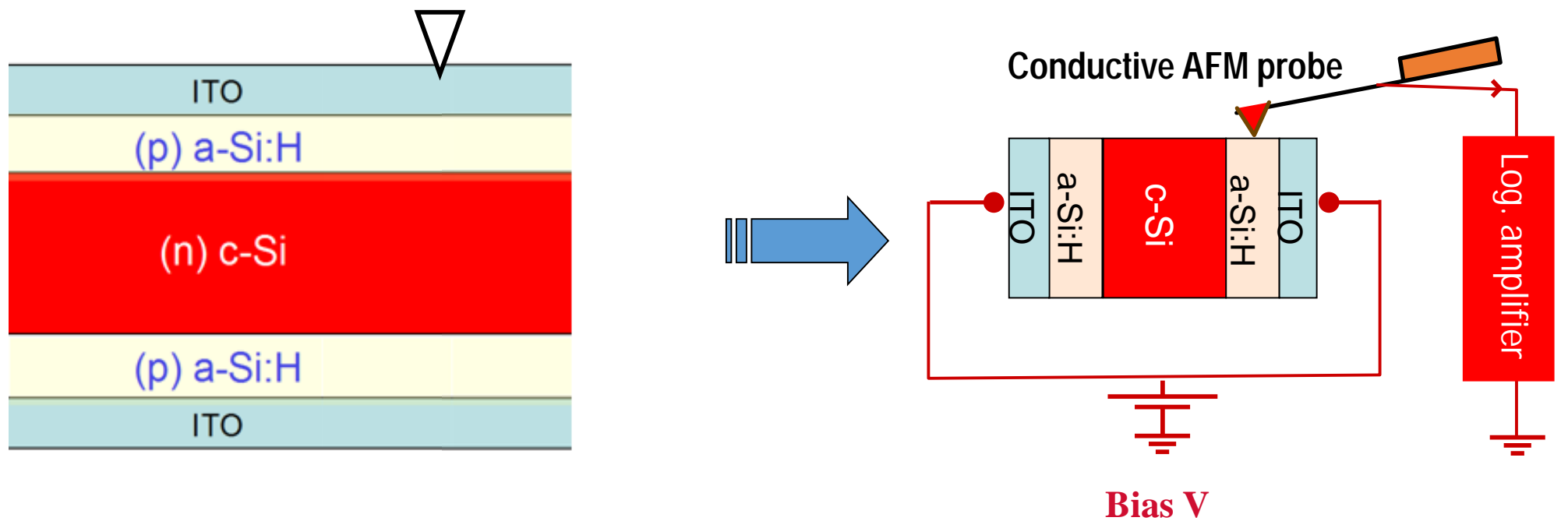


§ Considering the different current pathways only the high conductance at the a-Si:H/c-Si interface can explain the very low E_A of the Arrhenius plot.

1.3 Conductive-AFM (C-AFM) approach (1/3)

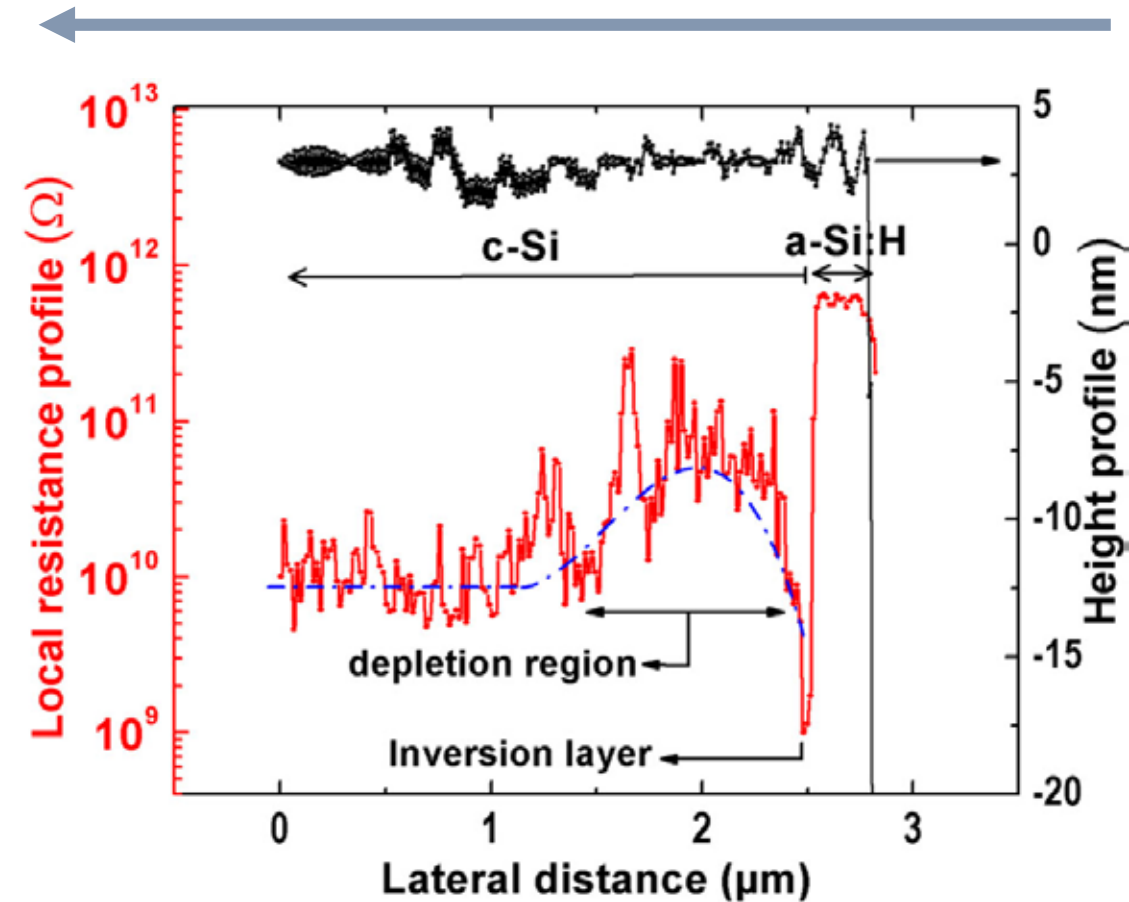
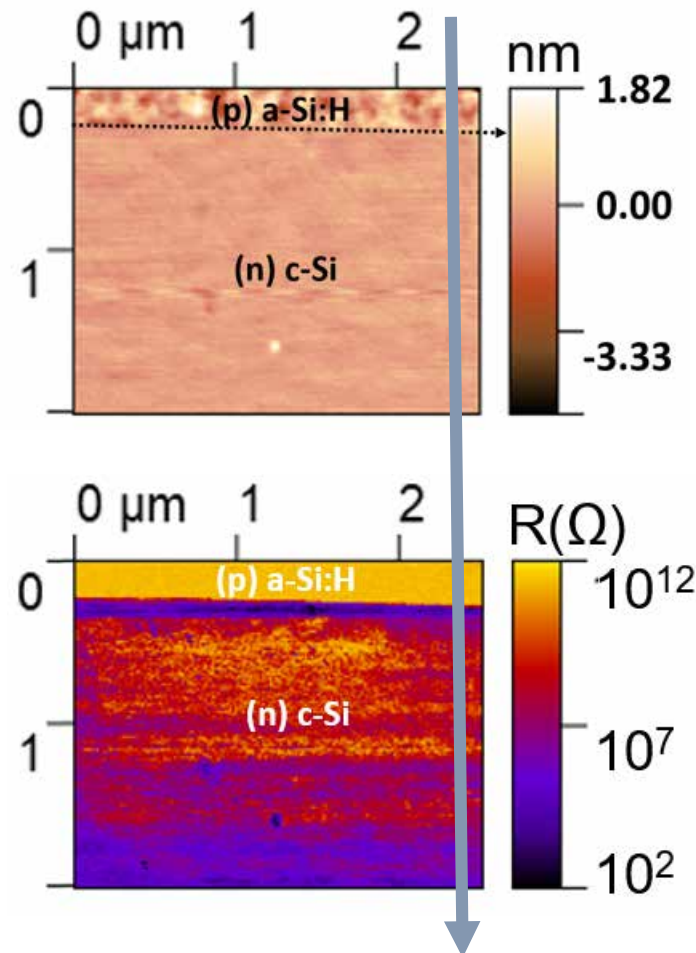
§ Sample preparation for cross-sectional investigations

- Cleavage and HF (1%) trench dipping



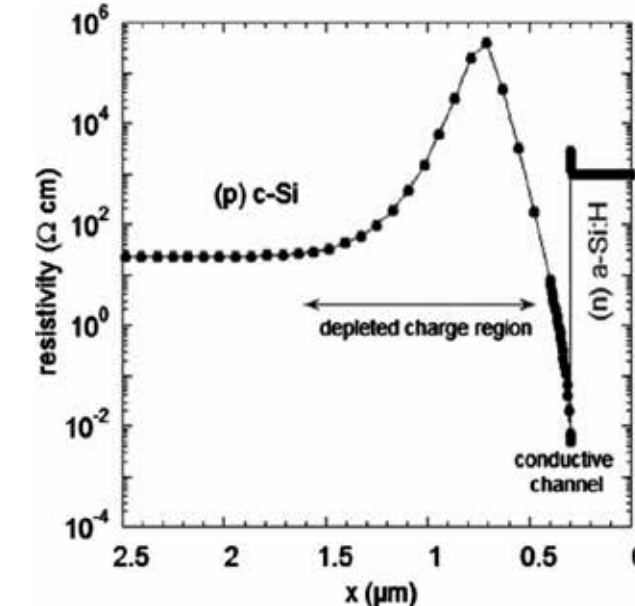
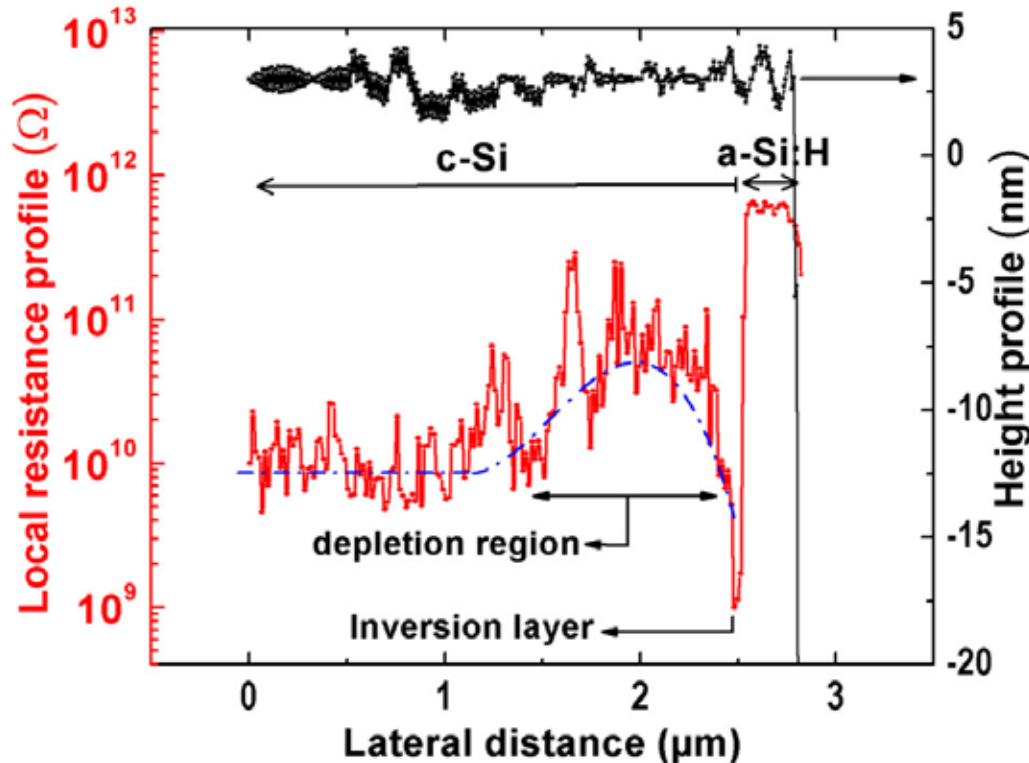
1.3 Conductive-AFM (C-AFM) approach (2/3)

§ Cross-sectional mapping



1.3 Conductive-AFM (C-AFM) approach (3/3)

§ Comparison b/w experimental C-AFM and modelling AFORS-HET



- Resistivity profile calculations confirm the qualitative C-AFM observations

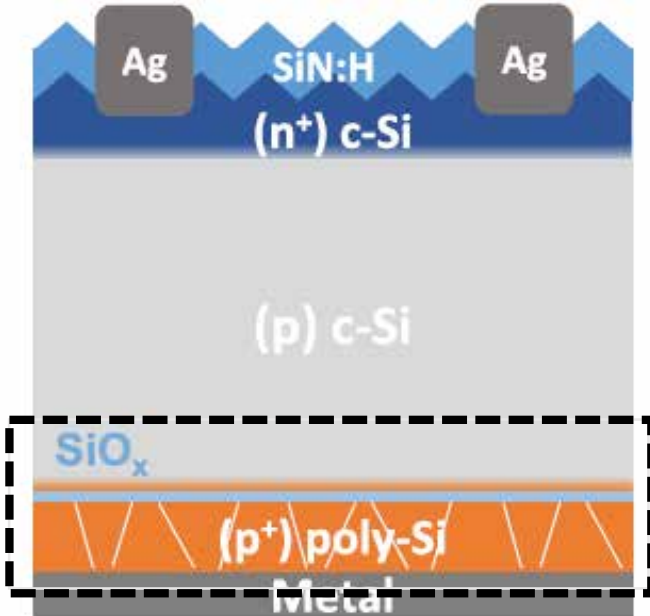
Part 1 - Hydrogenated amorphous silicon/crystalline silicon heterojunction

Part 2 - Passivating selective contacts: (p+) Poly-Si/SiO_x/c-Si

Part 3 - P-I-N radial junctions (RJ) Silicon Nanowires (SiNWs)

Part 2

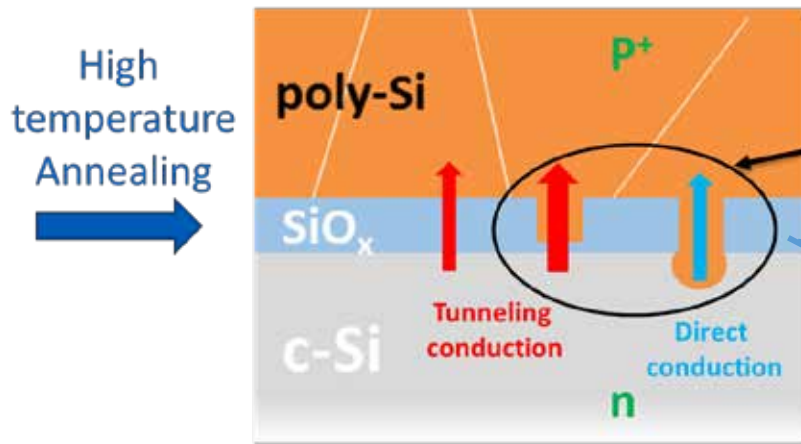
Passivating selective contacts: (p+) Poly-Si/SiO_x/c-Si



- § Poly-Si passivating contact studied in the 80's [1,2]
- § 2016 – present : Intensively studied by many research groups (Fraunhofer ISE, ISFH, NREL, INES-CEA...)
 - è Reduce back contact recombination losses reaching efficiencies in the range 25-26.1% [3][4]

- [1] Yablonovitch et al., *APL* 47(11), 1211–1213 (1985)
- [2] Van Halen et al., *IEEE Trans. Elec. Dev.* 32(7), 1307–1313 (1985)
- [3] Richter et al., *Sol. Energy Mater. Sol. Cells* 173, 96–105 (2017)
- [4] Haase et al., *Sol. Energy Mater. Sol. Cells* 186, 184–193 (2018)

2.1 Motivation : conduction mechanisms across the structure?



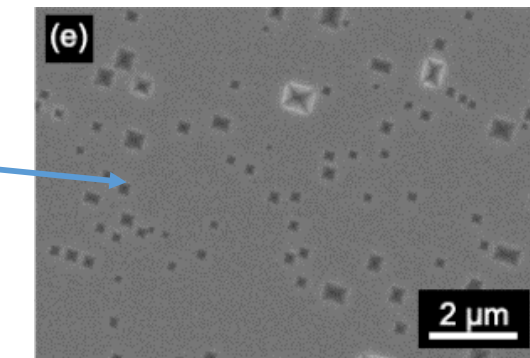
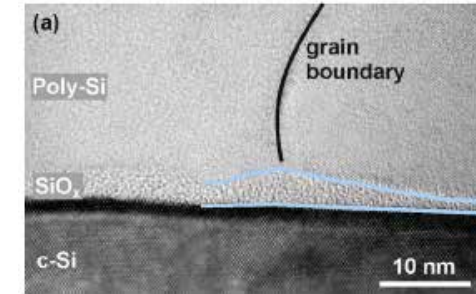
High temperature Annealing

TEM : thinner oxide

Chemical etching : nano-holes

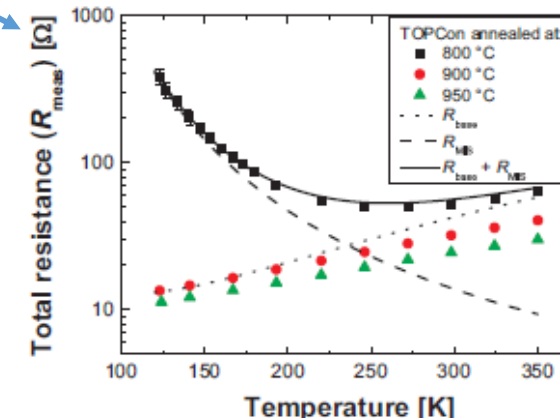
$R = f(T)$

Transport mechanism



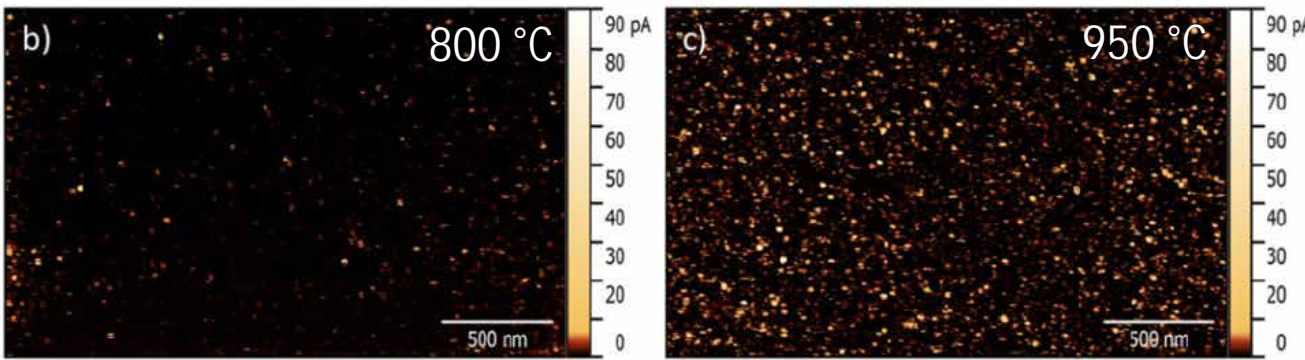
Peibst et al.,
Solar energy
materials and
solar cells 158,
60-67 (2016)

Wietler et al., Appl.
Phys. Lett. 110,
253902 (2017)

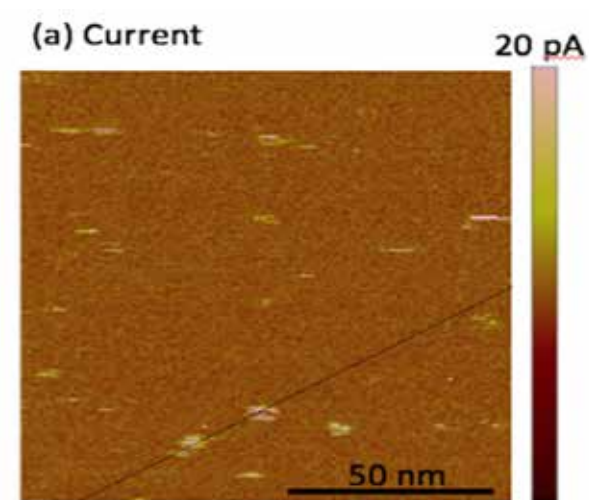


Feldmann et al., Solar
energy materials and solar
cells 178, 15-19 (2018)

2.2 Conductive –AFM (C-AFM) approach

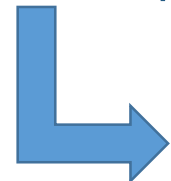


- Lancaster et al., Energy procedia 92, 116-121 (2016)



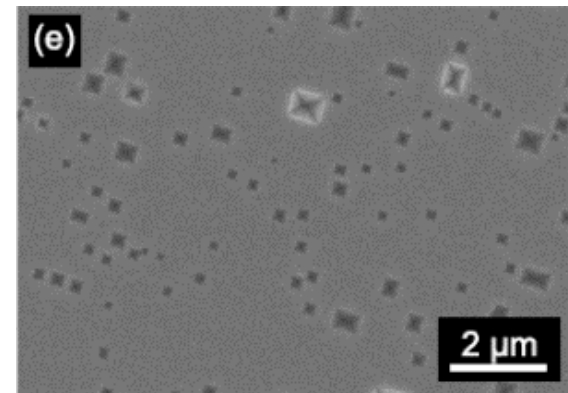
Zhang et al., Sol. Energy Mater. Sol. Cells 187, 113-122 (2018)

§ Conductive Spots =degraded oxide= pinholes $\sim 250 - 750 \mu\text{m}^{-2}$



"Inconsistent with the selective etching approach"

Pinholes density $\sim 0.1-2 \mu\text{m}^{-2}$

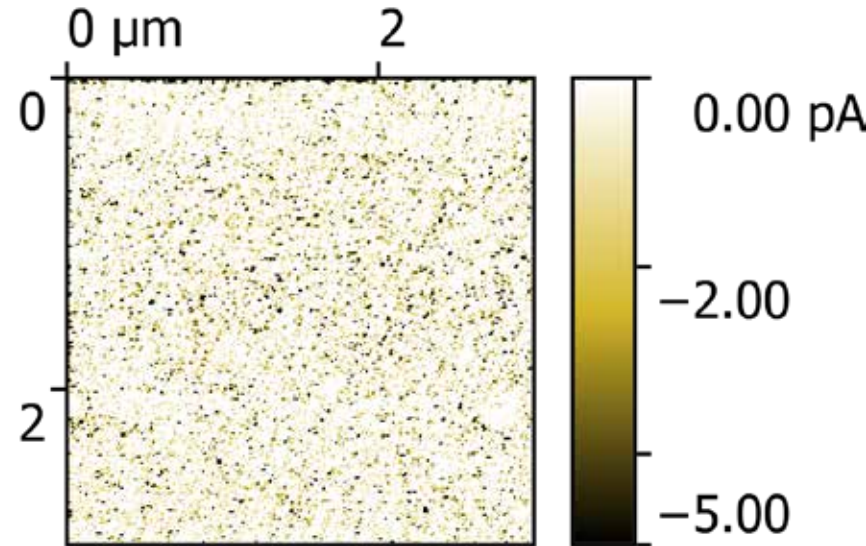


§ Lack of understanding of the C-AFM measurement !

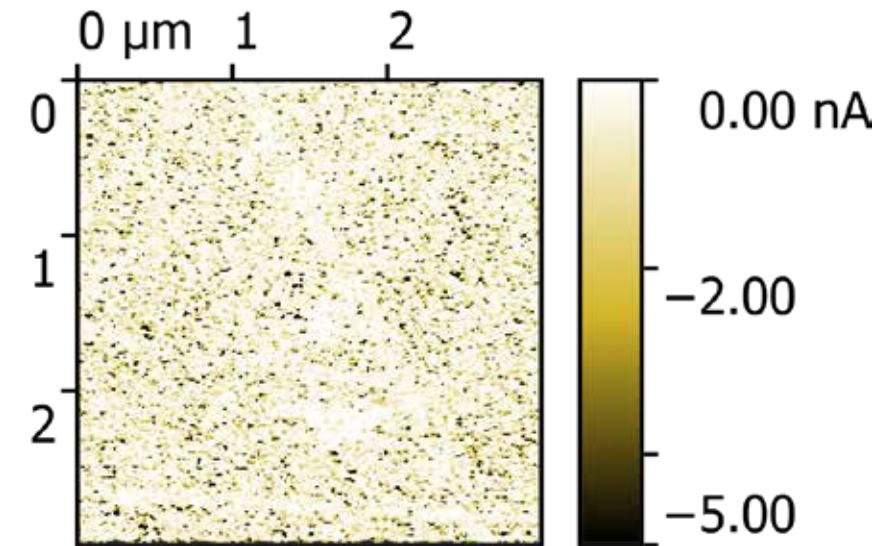
Wietler et al., Appl. Phys. Lett. 110, 253902 (2017)

2.3 C-AFM : new experiments on (p+) poly-Si/SiO_x/c-Si (n) (1/3)

§ C-AFM versus surface preparation



“No surface preparation” :
pA current peak levels

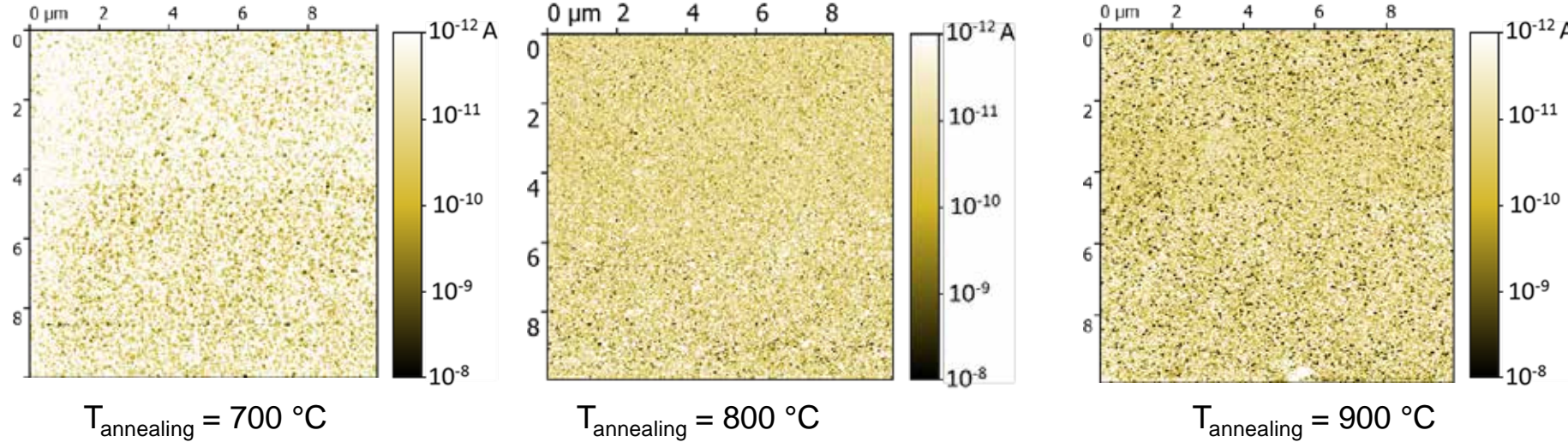


“Surface HF (1%) treated” :
nA current peak levels

- Deoxidation of the poly-Si surface is a requirement

2.3 C-AFM : new experiments on (p+) poly-Si/SiO_x/c-Si (n) (2/3)

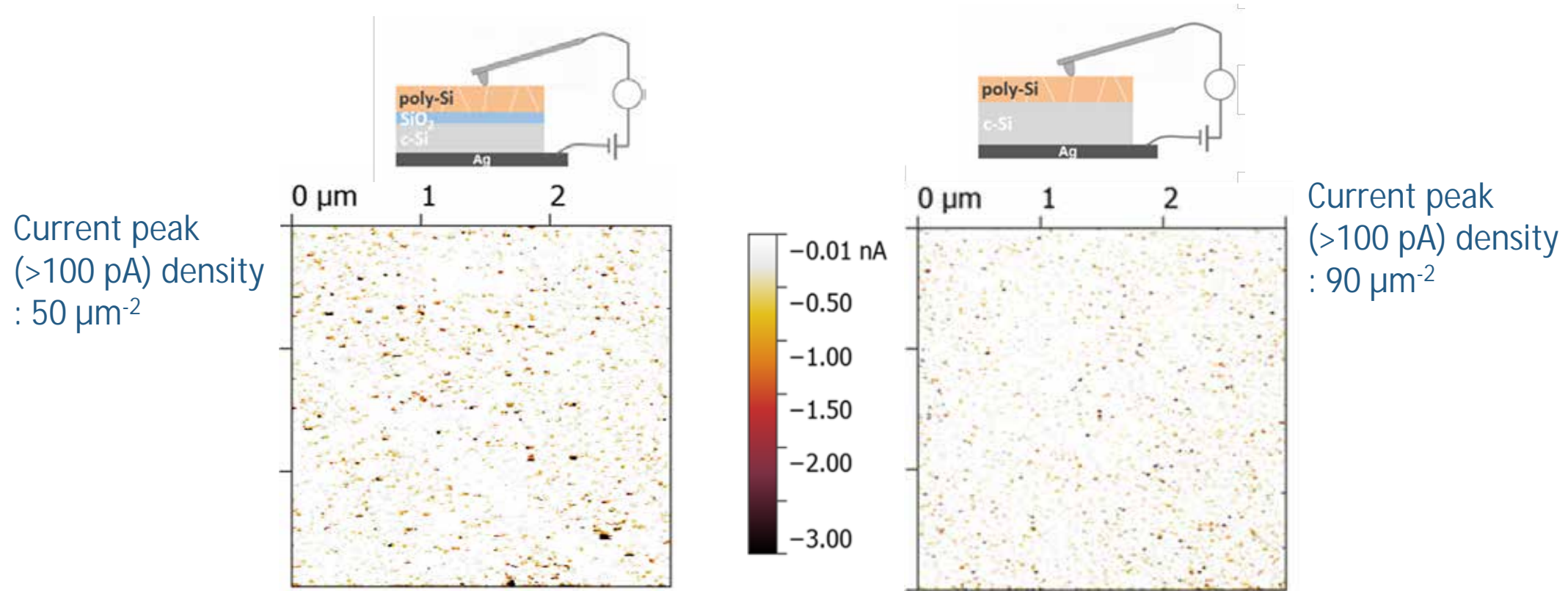
§ C-AFM versus annealing temperature



- Current peaks (CP) > 100 pA, densities ~10-100 μm⁻²
- è C-AFM does not allow to discriminate the conduction through the pinholes

2.3 C-AFM : new experiments on (p+) poly-Si/SiO_x/c-Si (n) (3/3)

§ C-AFM with and without passivating oxide

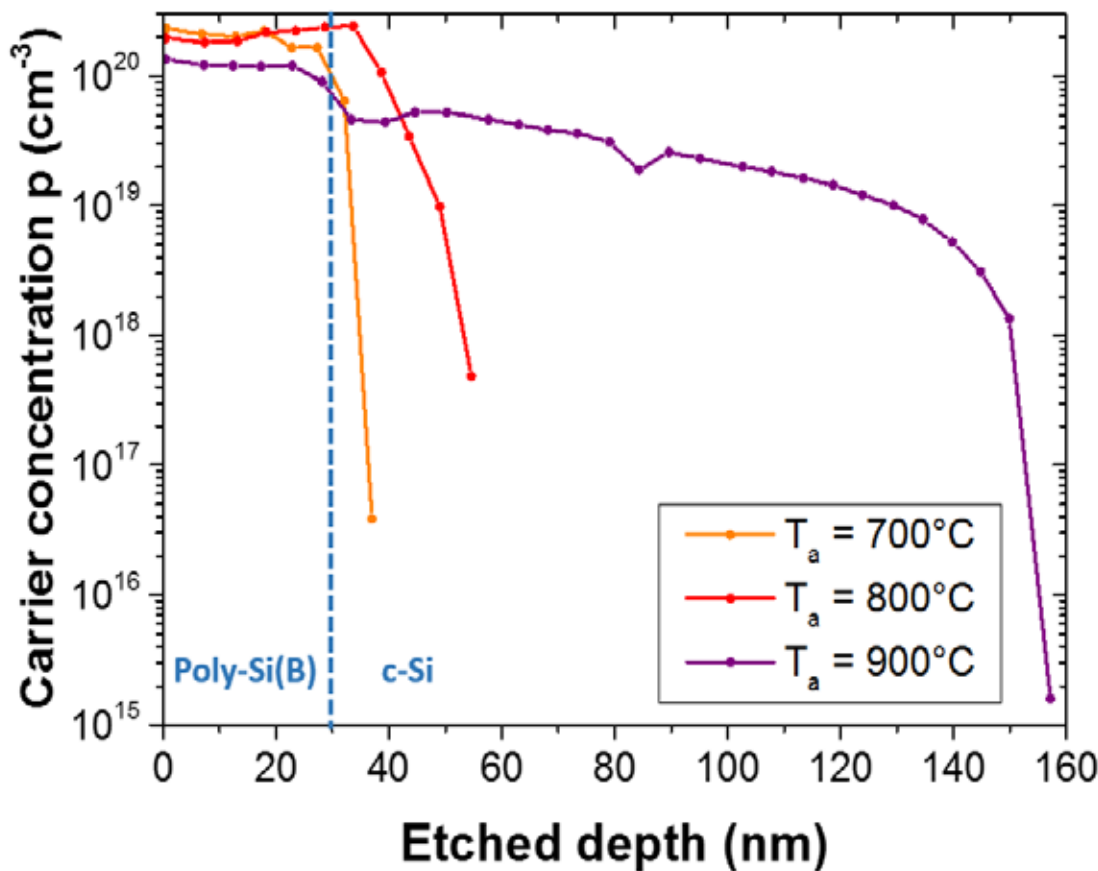


è C-AFM reflects poly-Si conduction inhomogeneities (surface morphology, doping...)

2.4 KPFM : new approach for (p+) poly-Si/SiO_x/c-Si (1/3)

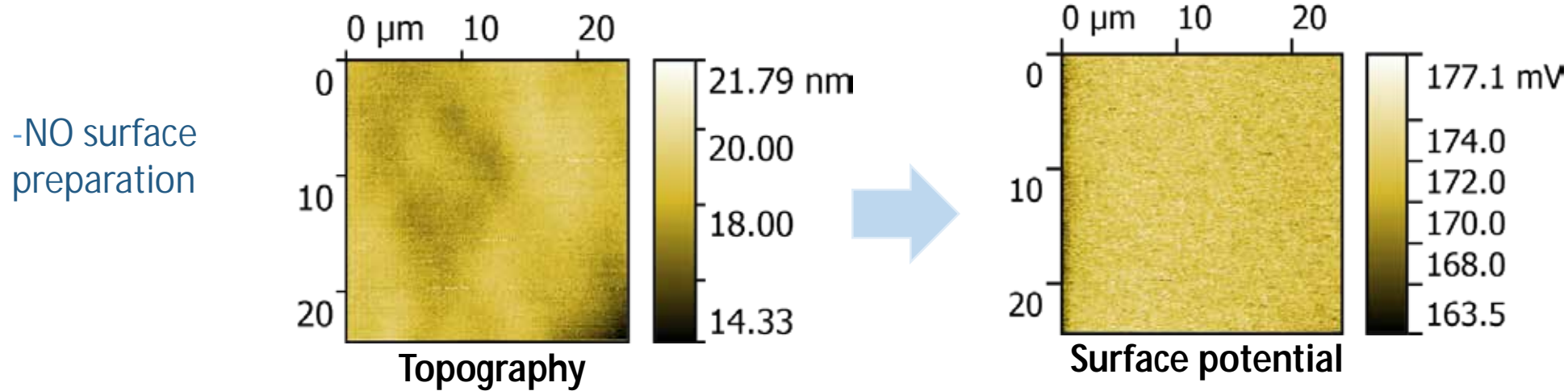
§ KPFM sensitive to the workfunction and the doping

§ ECV measurements on (p+) poly-Si/SiO_x/c-Si



2.4 KPFM : new approach for (p+) poly-Si/SiO_x/c-Si (1/3)

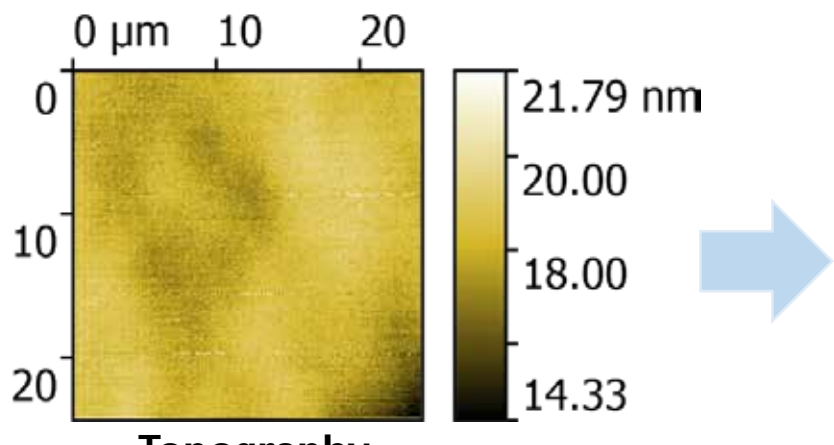
§ KPFM sensitive to the workfunction and the doping



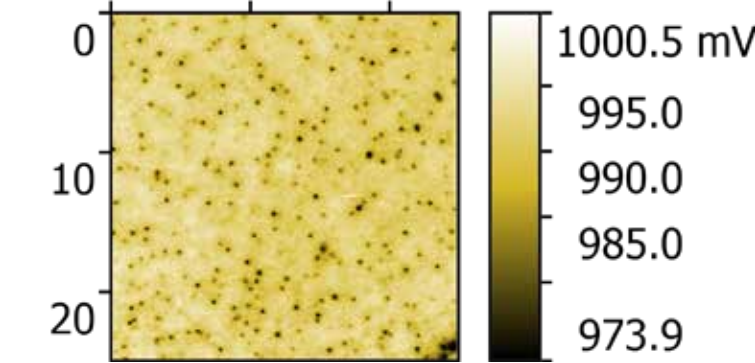
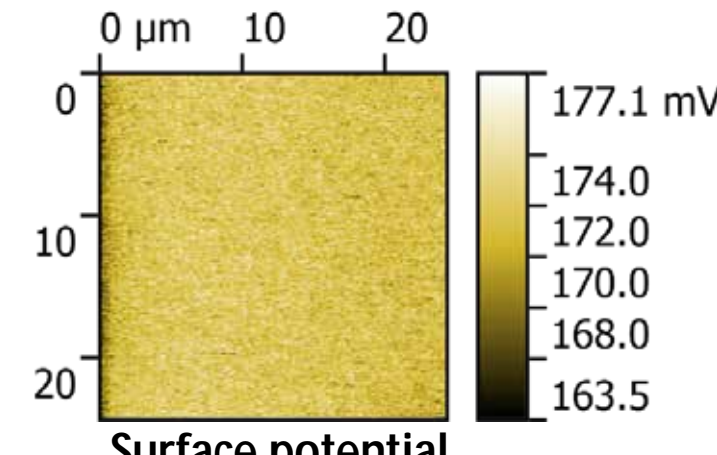
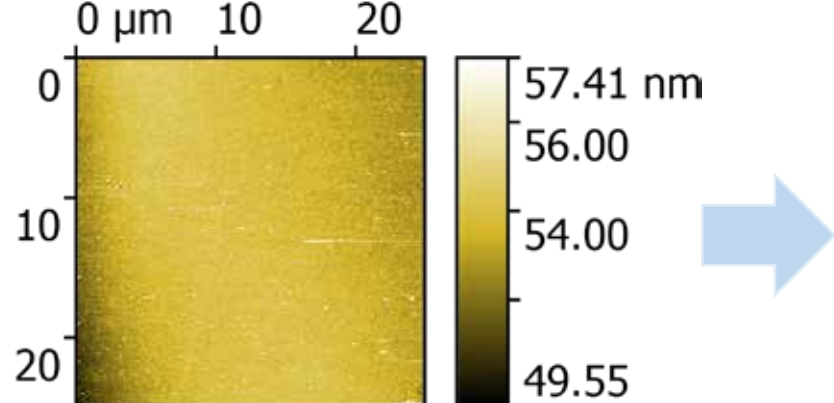
2.4 KPFM : new approach for (p+) poly-Si/SiO_x/c-Si (1/3)

§ KPFM sensitive to the workfunction and the doping

-NO surface preparation



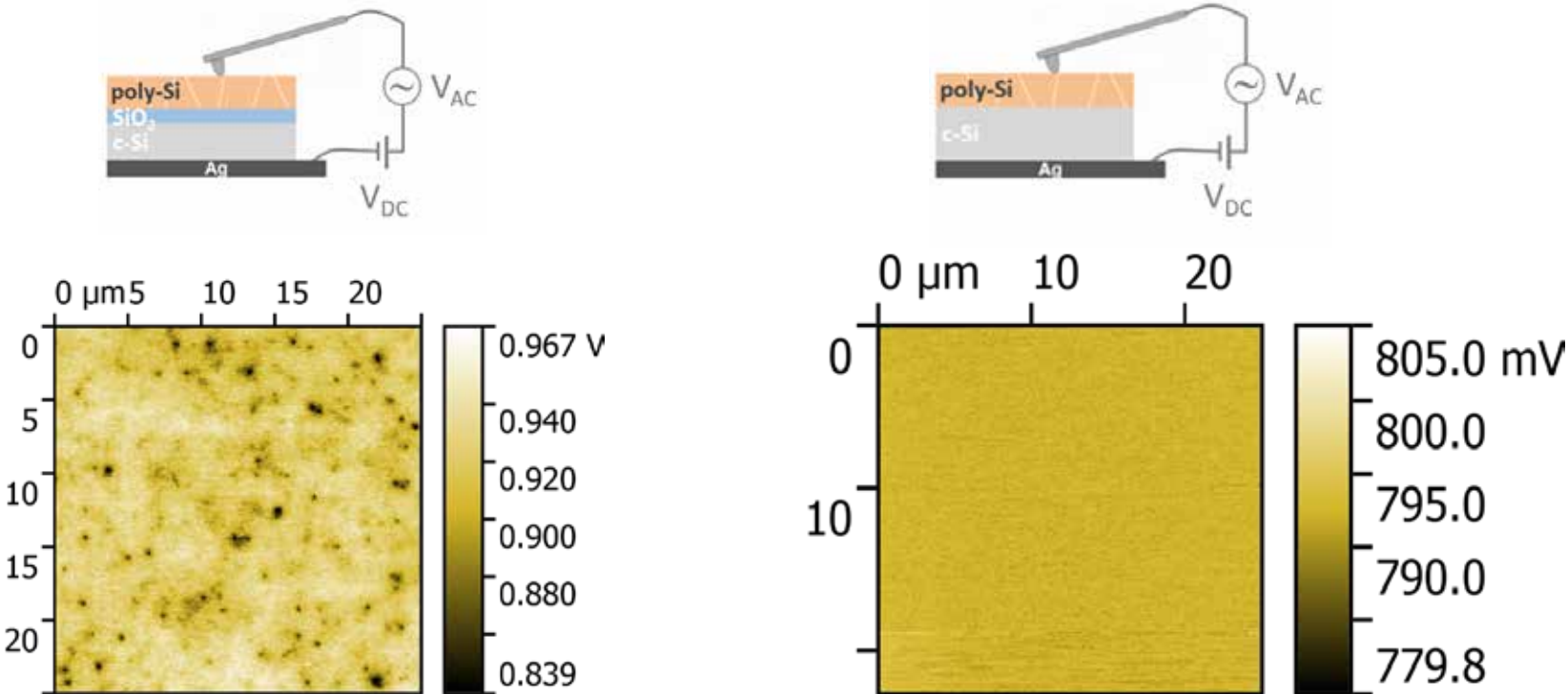
-After poly-Si surface deoxidation



- Deoxidation minimizes screening effects : potential drops on the poly-Si surface => Indirect pinhole observation ?

2.4 KPFM : new approach for (p+) poly-Si/SiO_x/c-Si (2/3)

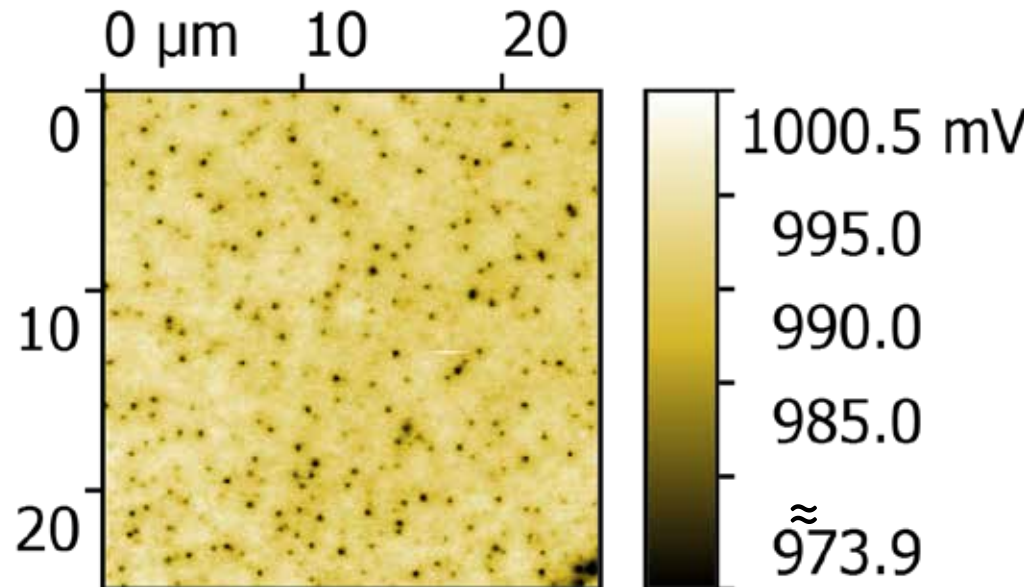
§ KPFM with and without passivating oxide



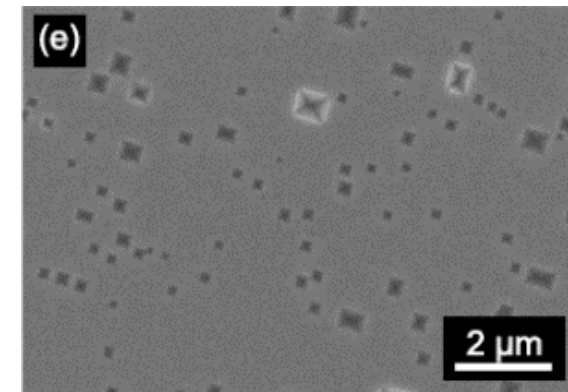
- Local potential drops observed **only with passivating oxide**

2.4 KPFM : new approach for (p+) poly-Si/SiO_x/c-Si (3/3)

§ KPFM and potential drops density



Potential drops density : 0.2 – 0.5 μm^{-2}



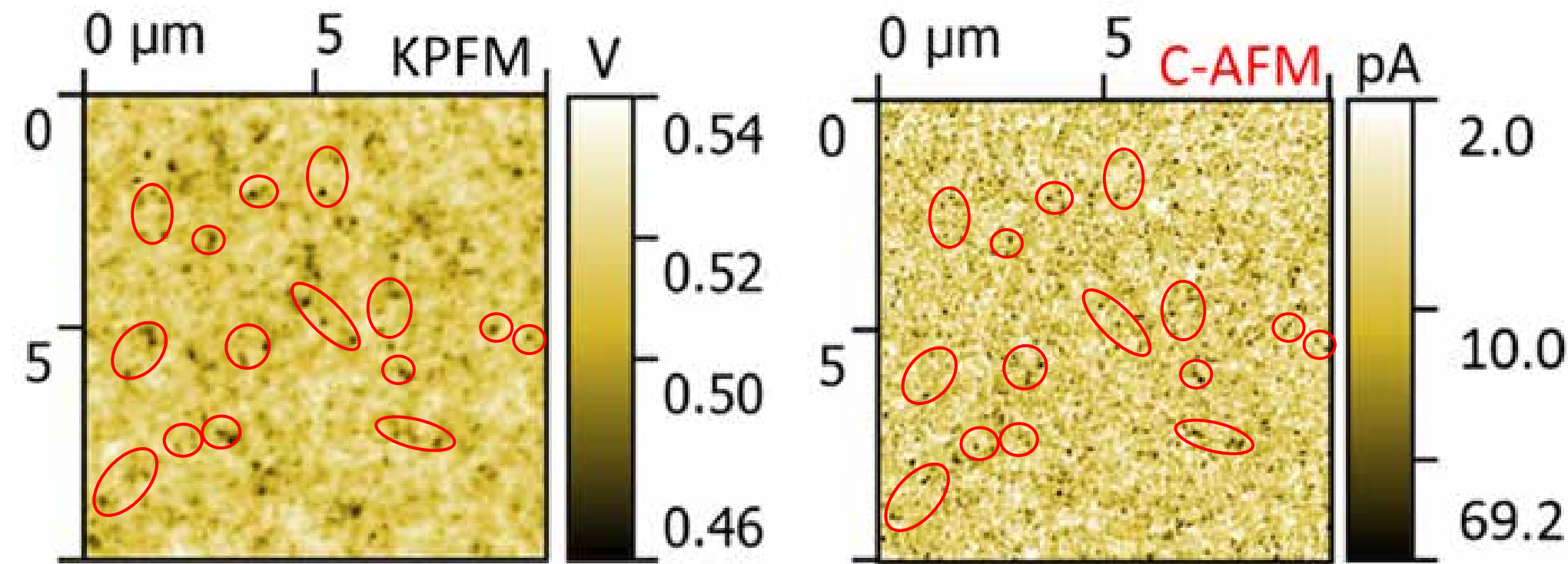
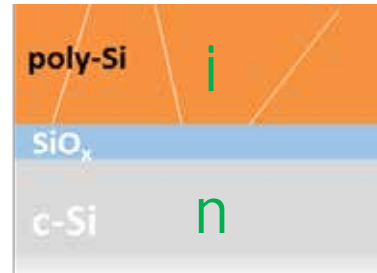
Wietler et al., *Appl. Phys. Lett.*
110, 253902 (2017)

Pinholes density ~ 0.1-2 μm^{-2}

-Potential drops density similar to literature pinhole density by selective chemical etching

2.5 Correlative C-AFM and KPFM on intrinsic Poly-Si/SiO_x/c-Si

§ Sample with an intrinsic top poly-Si layer



- Some local potential drops correlate well with current peaks (CPs)
- CAFM CPs reflect here conduction heterogeneities including the pinholes
- Correlations were possible due to the intrinsic layer that minimizes lateral conduction

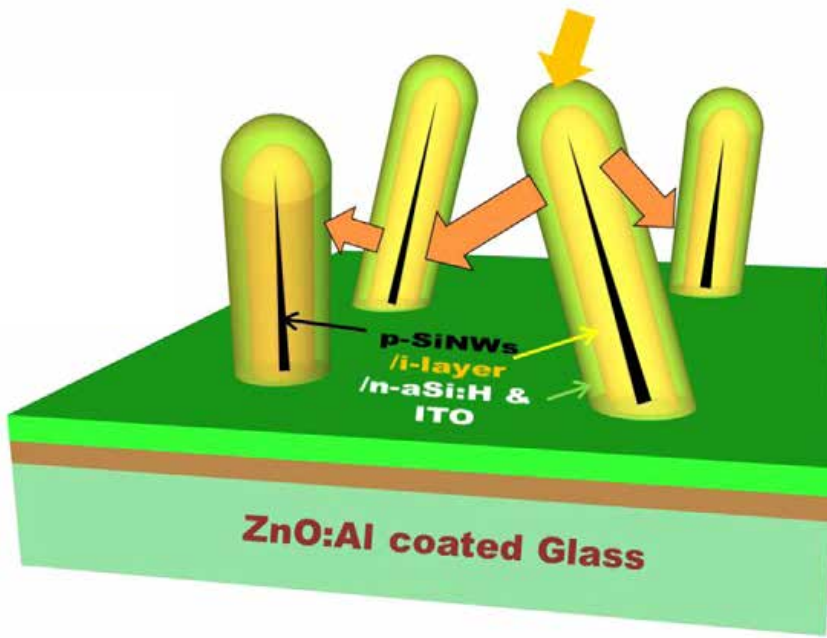
Part 1 - Hydrogenated amorphous silicon/crystalline silicon heterojunction

Part 2 - Passivating selective contacts: (p+) Poly-Si/SiO_x/c-Si

Part 3 - P-I-N radial junctions (RJ) Silicon Nanowires (SiNWs)

Part 3

P-I-N radial junctions (RJ) Silicon Nanowires (SiNWs)



[1] Misra et al., IEEE JPV 5(1), 40–45 (2015).

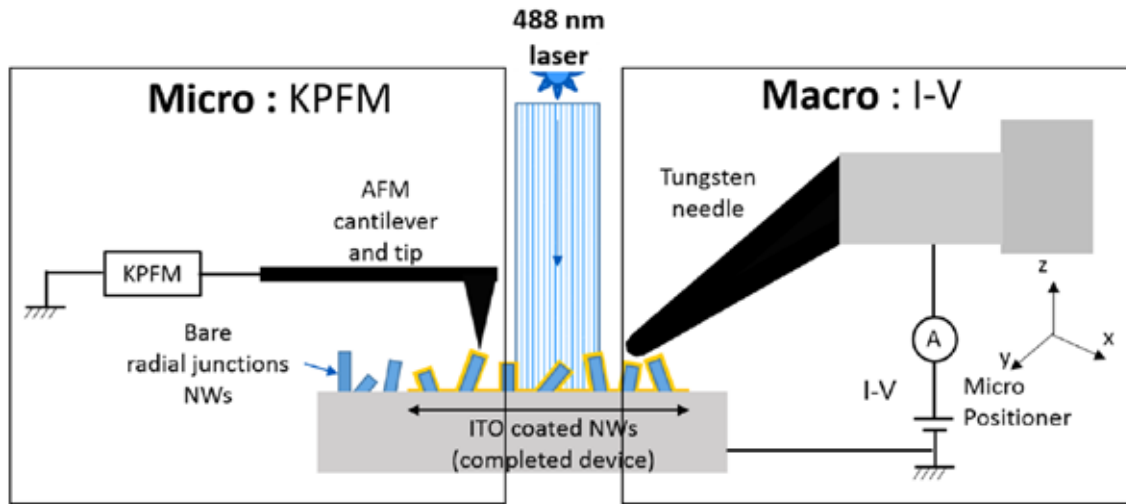
- § NWs promising route for enhancing solar performances : less material; more efficient separation/collection of photocarriers
- § RJ technology “orthogonalizes” the light absorption and the minority carrier collection
- § Highly doped SiNWs grown by VLS using Sn catalysts with conformal deposition of (i) and (n) a-Si:H, and ITO.
- § Efficiencies up to 9.6% [1] have been demonstrated
- § Improvements require a better understanding of the individual nanodevice

3.1 Evaluation of local open-circuit voltage on single RJ SiNW by KPFM

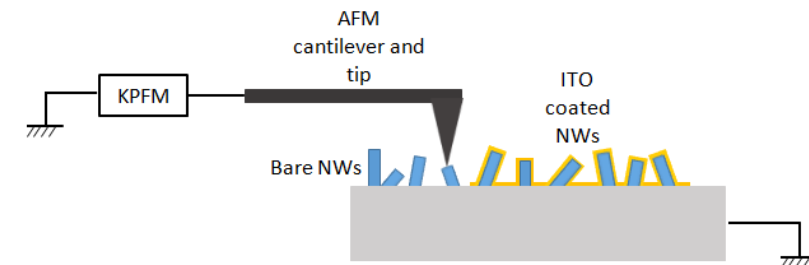
§ Surface PhotoVoltage (SPV) very effective technique to image the V_{OC} of solar cells

§ 1st approach, SPV extracted by KPFM on completed devices and comparison with V_{OC} by I-V

§ 2nd approach, SPV measurements by KPFM (only) on isolated RJs where the SiNW device



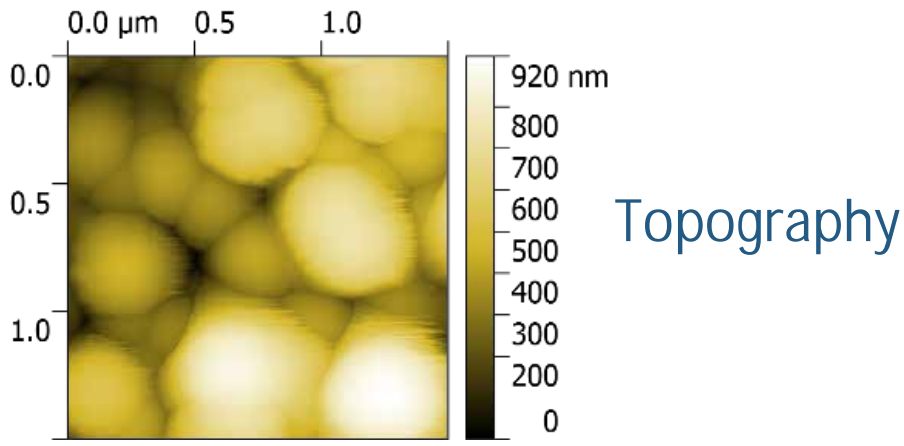
1st approach on completed devices



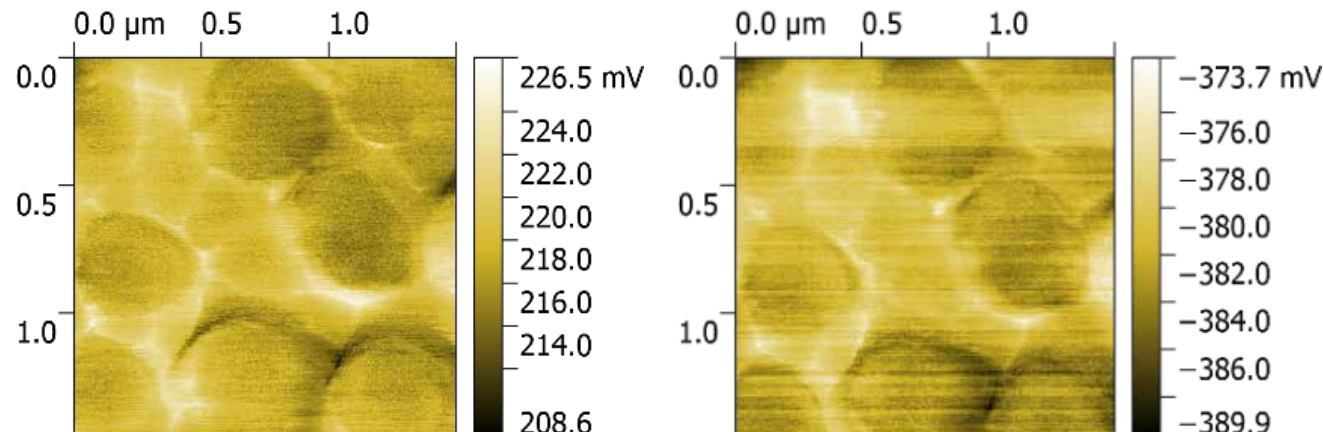
2nd approach on single RJs without ITO

3.2 1st approach : KPFM and I-V measurement analysis (1/2)

KPFM



Topography

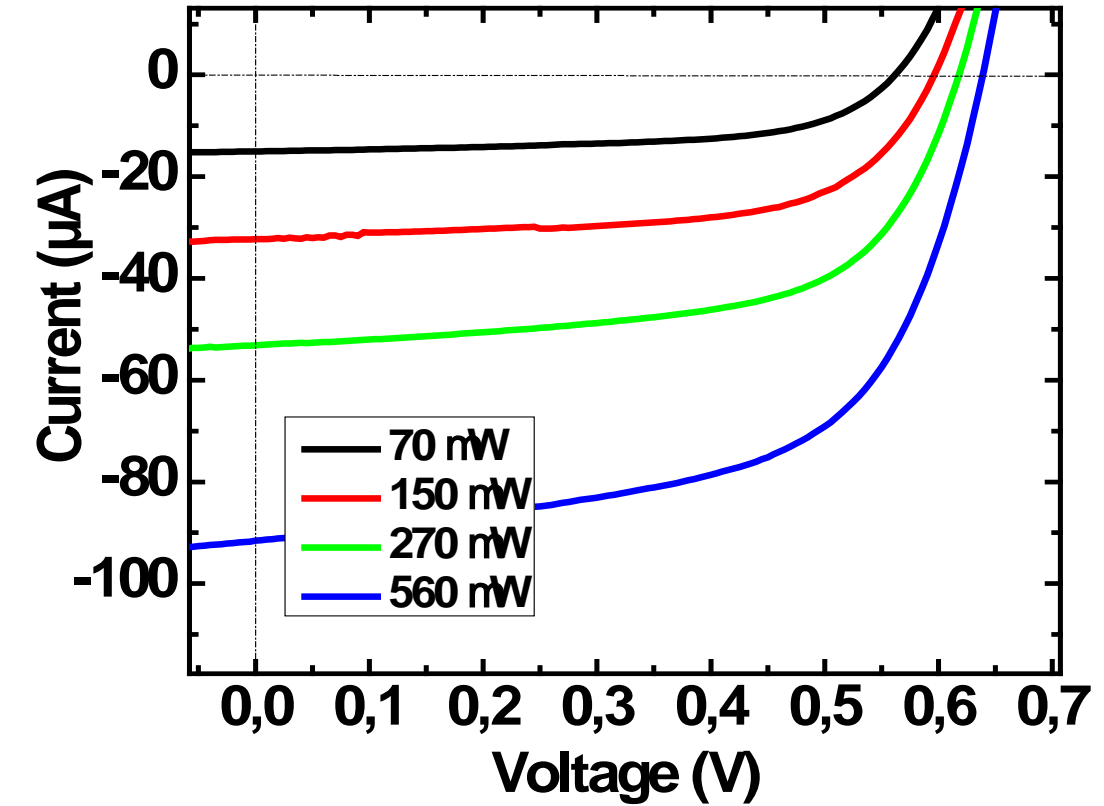


CPD dark

CPD illumination

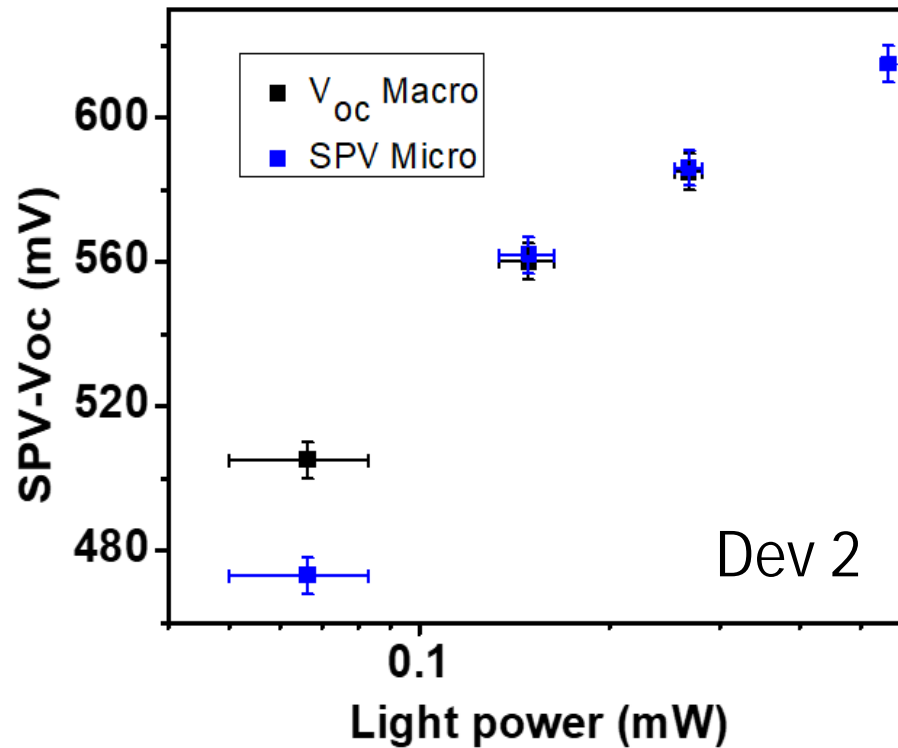
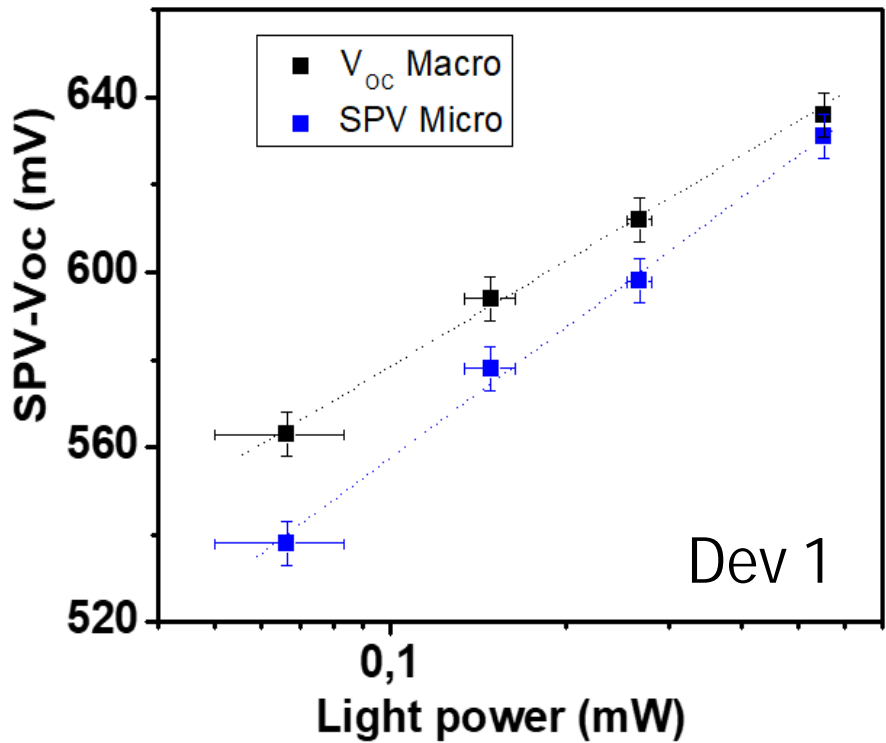
$$\frac{1}{2}SPV = CPD_{illu} - CPD_{dark}$$

Macro I-V



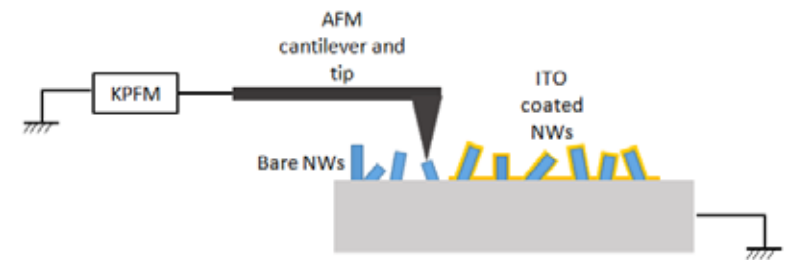
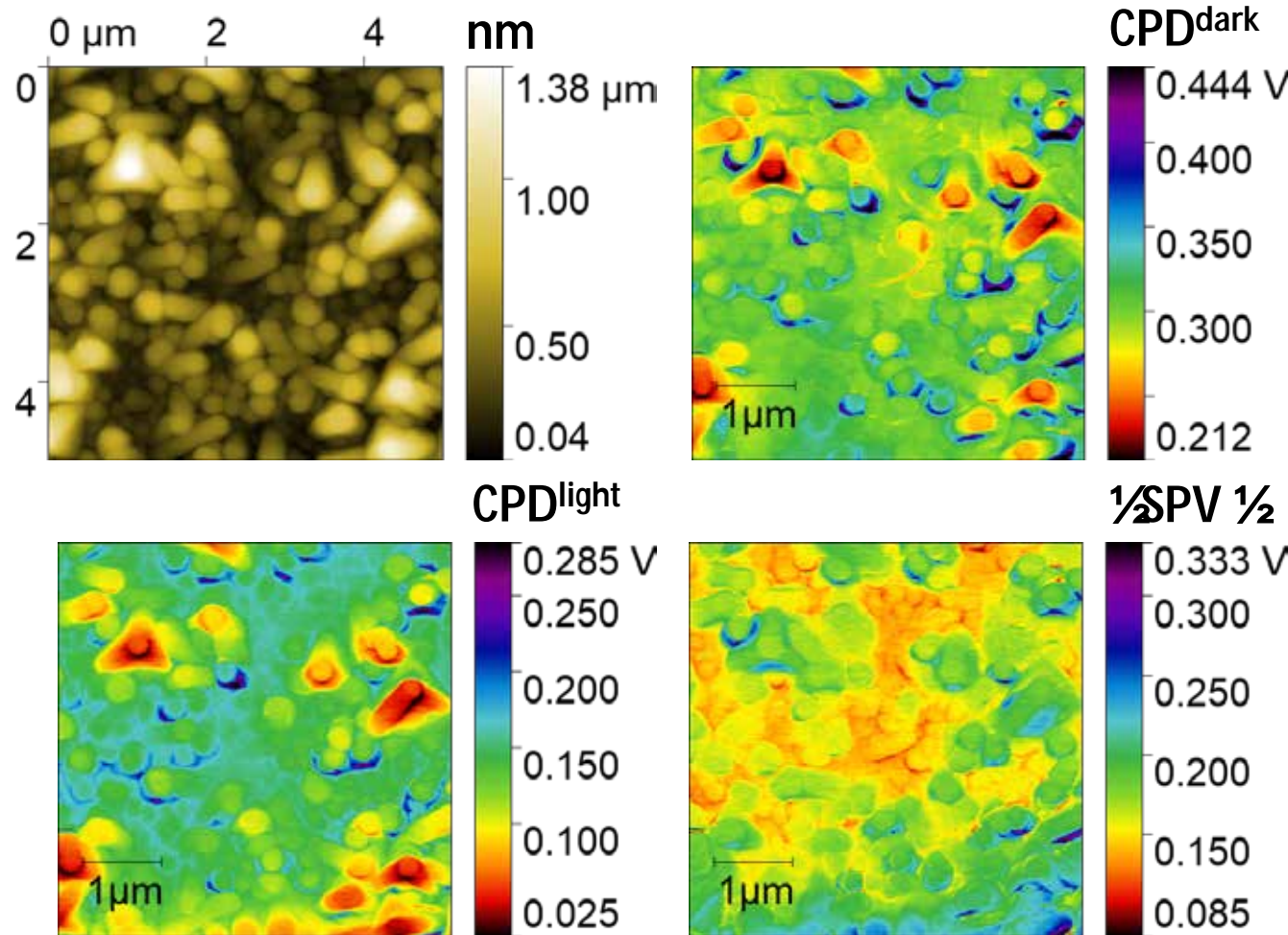
3.2 1st approach : KPFM and I-V measurement analysis (2/2)

§ V_{OC} and SPV versus light power for two different devices



- SPV and V_{OC} show linear behavior versus light power (log scale) with max. deviation b/w 2-5%.
- Ideality factor n : 1.5 ± 0.1 (dev. 1) and 1.75 ± 0.25 (dev.2) in line with a-Si:H planar devices

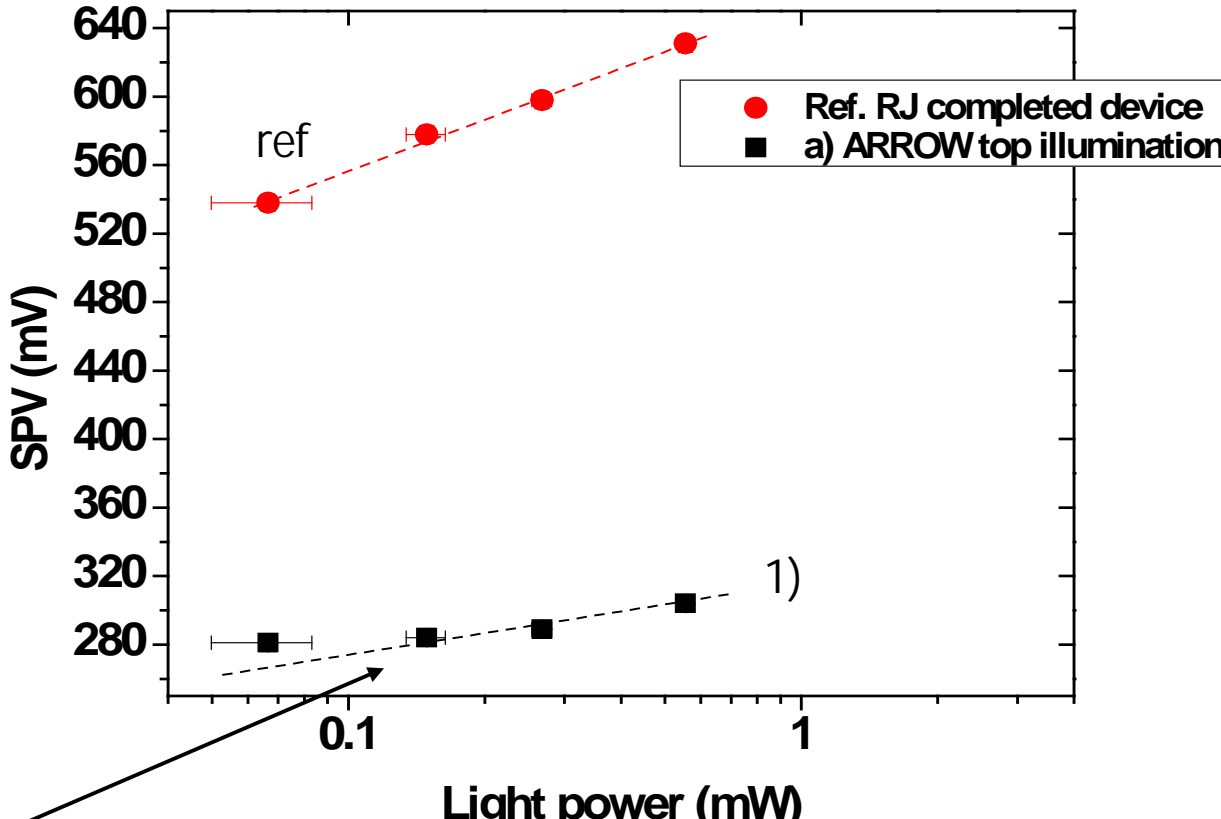
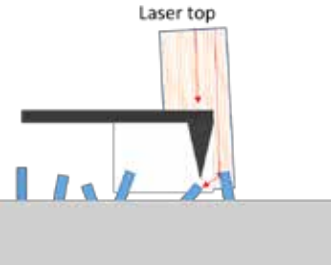
3.3 2nd approach : KPFM on single, isolated RJs (1/3)



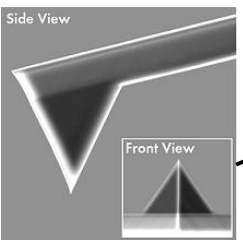
- Lowest SPV are observed in regions where the NWs appear the smallest

3.3 2nd approach : KPFM on single, isolated RJs (2/3)

Top illumination



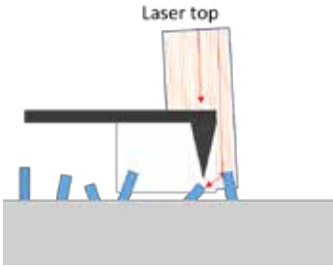
Conventional AFM
tip shape



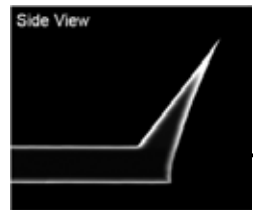
1)

3.3 2nd approach : KPFM on single, isolated RJs (2/3)

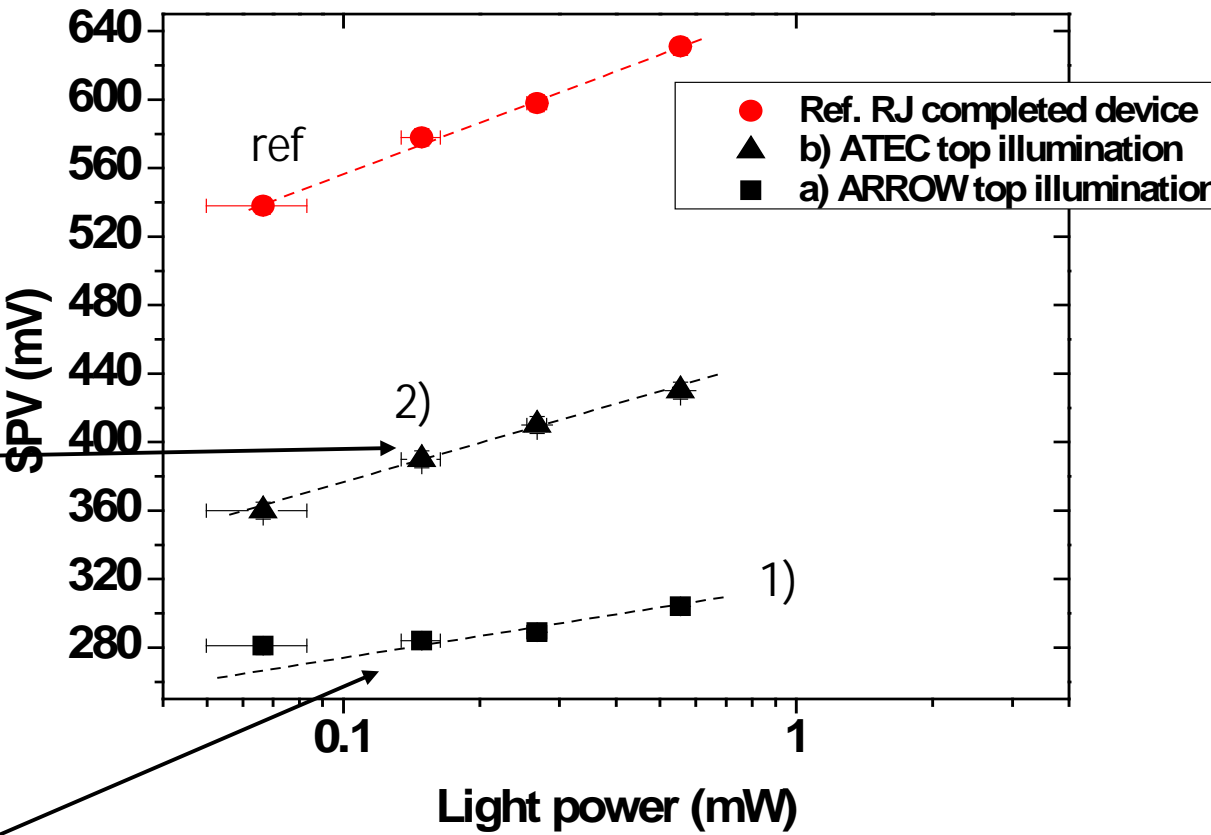
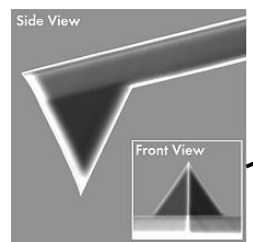
Top illumination



AFM tilted tip

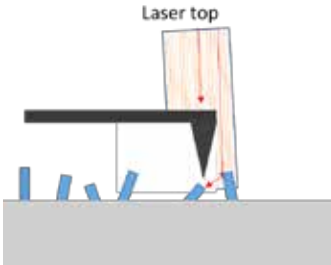


Conventional AFM tip shape

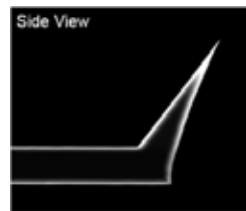


3.3 2nd approach : KPFM on single, isolated RJs (2/3)

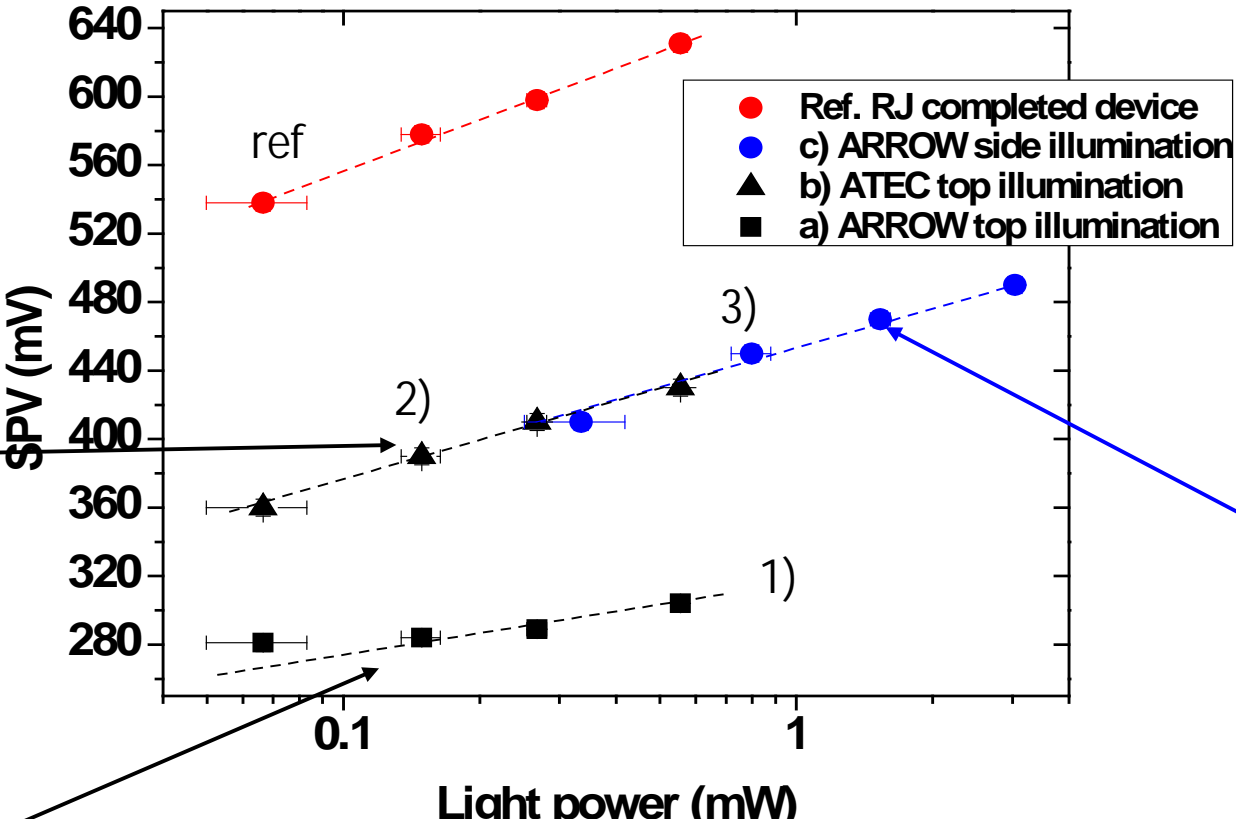
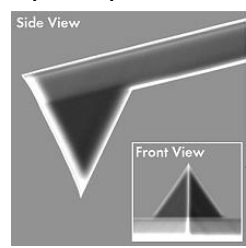
Top illumination



AFM tilted tip

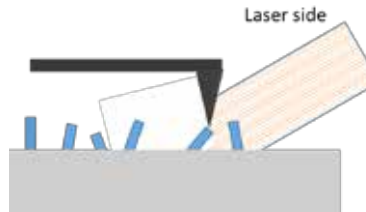


Conventional AFM tip shape

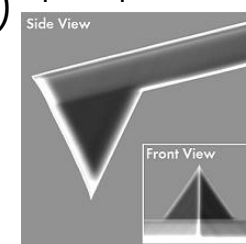


- SPV value on single Si NW RJ never reached the reference SPV

Side illumination

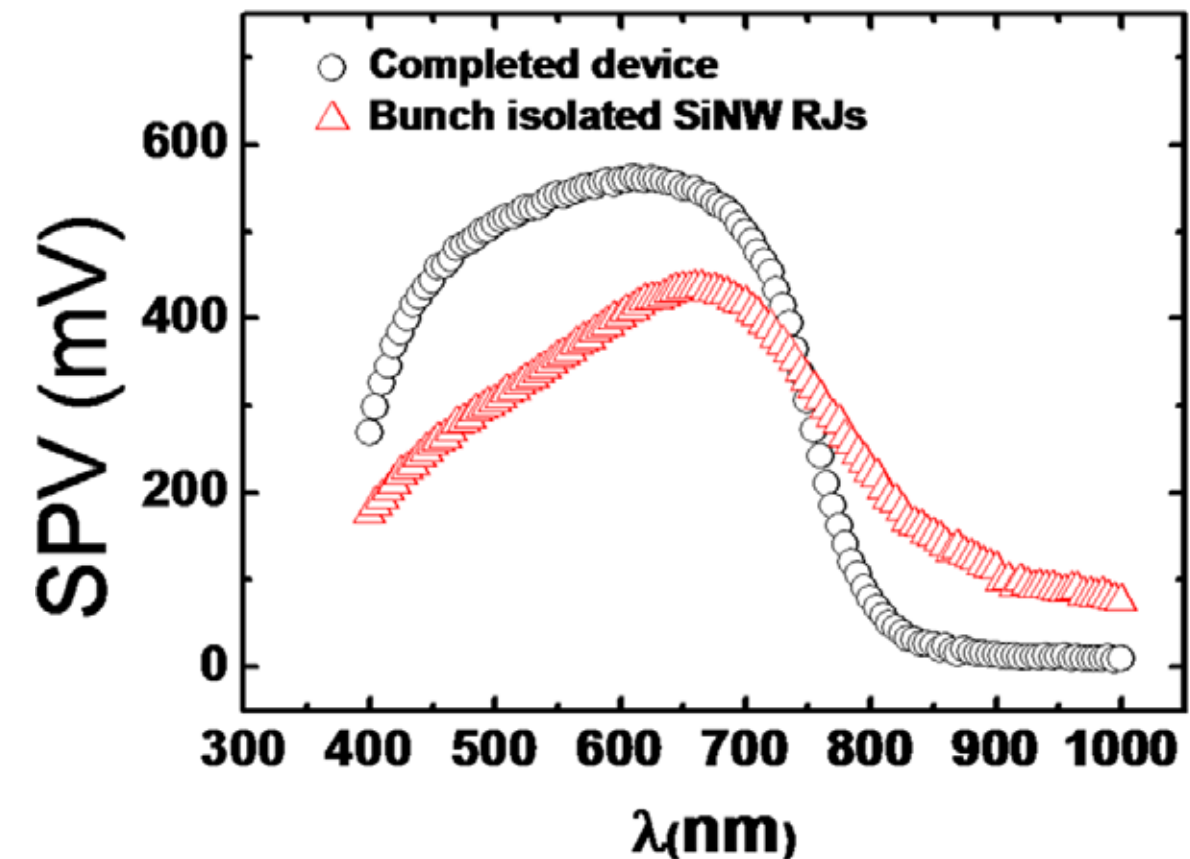


Conventional AFM tip shape



3.3 2nd approach : KPFM on single, isolated RJs (3/3)

§ Surface photovoltage Spectroscopy (SPS)



- SPS curves show large differences :
- w/o ITO “single, isolated SiNW RJ” cannot reflect the optimal V_{OC} value
- SPV is here impacted by a band-bending at the surface (no FB conditions) linked to defects or dipoles formation

Conclusion

Electrical AFM provides a unique chance to measure local properties of matter and characterize interfaces, junction and nanodevices.

- § Cross-sectional analysis applied on a-Si:H/c-Si allow to confirm the presence of the inversion layer suggested by macroscopic measurements.
- § C-AFM is not the best approach to investigate (p+) Poly-Si/SiO_x/c-Si. KPFM allows to observe local potential drops that are expected to be an indirect observation of the dopant diffusion through the existing pinholes.
- § SPV measurements by KPFM allows to get access to the V_{OC} in P-I-N RJ SiNWs only on completed devices. W/o ITO “single, isolated SiNW RJ” cannot reflect the optimal V_{OC} due that surface band bending negatively impacts SPV measurement.

Acknowledgements



- Delfina Muñoz
- Sébastien Dubois
- Thibaut Desrues



- Christophe Bonelli



- SOLARIUM (ANR-14-CE05-0025)
- OXYGENE (ANR-17-CE05-0034)



- Martin Foldyna
- Soumyadeep Misra



- Marie Gueunier-Farret
- Rudi Brüggemann
- Sylvain Legall

Jose.Alvarez@centralesupelec.fr